Chapter 3

EXPERIMENTAL: SET-UP, PROCEDURE AND MATERIAL

3.0 Introduction

The distinctive advantages of advanced composites led to diversification and rise of the composite industry. Advanced composite performance can be achieved only through accurate selection of both the constituent: fiber reinforcements and the polymer matrix (resin) which binds them into a cohesive structural unit. The successful performance of a composite depends greatly on both constituent phases.

From the available literature, it is clear that properties of composites are affected by laying the fabric at different angle used for reinforcement [1-2,67-70,174-175]. The properties of the composites as engineered by hybridisation by using different lay-up and matrix to modify the function as demanded by application. The present study is confined to study the performance of the textile reinforced composites when fabric layers are oriented differently in terms of their angles, their basic structure (weave), hybridization and stacking sequence. To minimize impact on the cost, an attempt has been made to consider HDPE yarn for hybridization.

Commercially, woven Carbon fabrics are available with a standard set of warp and weft. Moreover, limited range of weave parameters are being marketed by the manufacturers. For this research, it was required different combination of fabric to study differently oriented layers.

To achieve the goal of this research work, different hybridised fabrics were prepared. Different hybridised fabrics such as Carbon-Carbon; Carbon-Kevlar and Carbon-HDPE were prepared for studying the effect of different orientation. Then, composites having differently oriented layers were manufactured by using hand lay-up techniques. The prepared textile composites having differently oriented layers of fabrics were analyzed by standard techniques for their physical, structural and mechanical properties.

3.1 Methodology

The methodology of experimentation adopted in this work is presented in three sections viz.,

Section I includes: Preparation of woven fabric with different parameters (warp yarn, weft yarn, threads/inch etc) and weaves (plain, twill, sateen). This section also comprises modification of CCI sample loom for effective weaving of Carbon, Kevlar and HDPE (high density polyethylene) fabric.

Section II includes: Preparation of textile composites using hand lay-up technique, by stacking the layers of hybrid fabrics differently at varied skew angles, weave structure and reinforcing yarn.

Section III includes: Testing and analysis of prepared hybridised composites for physical, structural, mechanical properties such as tensile, flexural, impact and damage resistance were done.

Section IV includes: Numerical evaluation of tensile strength of polymer textile composite laminate having different fabric layer orientation (different skew angle) using finite element method and Ansys software. This section has been described in Chapter 5.

SECTION - I

3.2 Weaving of hybrid fabric

The weaving of Carbon fabric normally is done commercially on a large-scale. The available Carbon fabrics are mainly with specific weave, thread counts and yarn parameters. This work required fabric having specific parameters like weave, yarn spacing and yarns were not available in the market. In this work, hybridised fabric with required weave and yarn parameters were prepared in the laboratory for research purpose. The hybrid fabric was prepared with *6K* x *12K* (K=1000) Carbon as *warp* x *weft*. Moreover, the hybridised fabric using HDPE yarn as warp having different weft line, Carbon and Kevlar, were prepared.

3.2.1 Materials

12K and 6K Carbon (in the form of tow) were purchased of reputed international company having the grade TC-36s and TC-35 respectively. Kevlar 49 yarn was also purchased from reputed manufacturer. HDPE yarn was obtained from local reputed company. The raw materials are shown in Figure 3.1.

Figure 3.1: Kevlar, Carbon, and HDPE yarn package (from L to R)

The important properties, required in this work were determined through the standard testing methods which are discussed in succeeding sections.

3.2.2 Experimental methods

The weaving procedure for Carbon, Kevlar and HDPE yarns to produce different types of fabric was commenced with the assistance of sample preparation machine:

(1) CCI single end warping machine

(2) CCI rapier sample loom.

Preparation of Carbon fabric was initiated on handloom to get the basic feel about the yarn's behavior on the sample loom.

3.2.2.1 Preparation of fabrics on sample loom

First, Handloom samples were prepared on handloom (Figure 3.2) to know the behaviour of yarn on before weaving on sample loom.

A. Preparation of sample on handloom

The beam having width 6" of 12K Carbon tow was prepared on the sectional warping machine using cotton yarn as selvedge. The first simple plain weave was prepared. After this different weave like twill (2/1 and 2/2) and 4 end sateen were prepared, some of them are shown in Figure 3.3. Many impediments like fraying and breaking of fibres were incurred during the weaving as envisaged.

Figure 3.2: Sample handloom

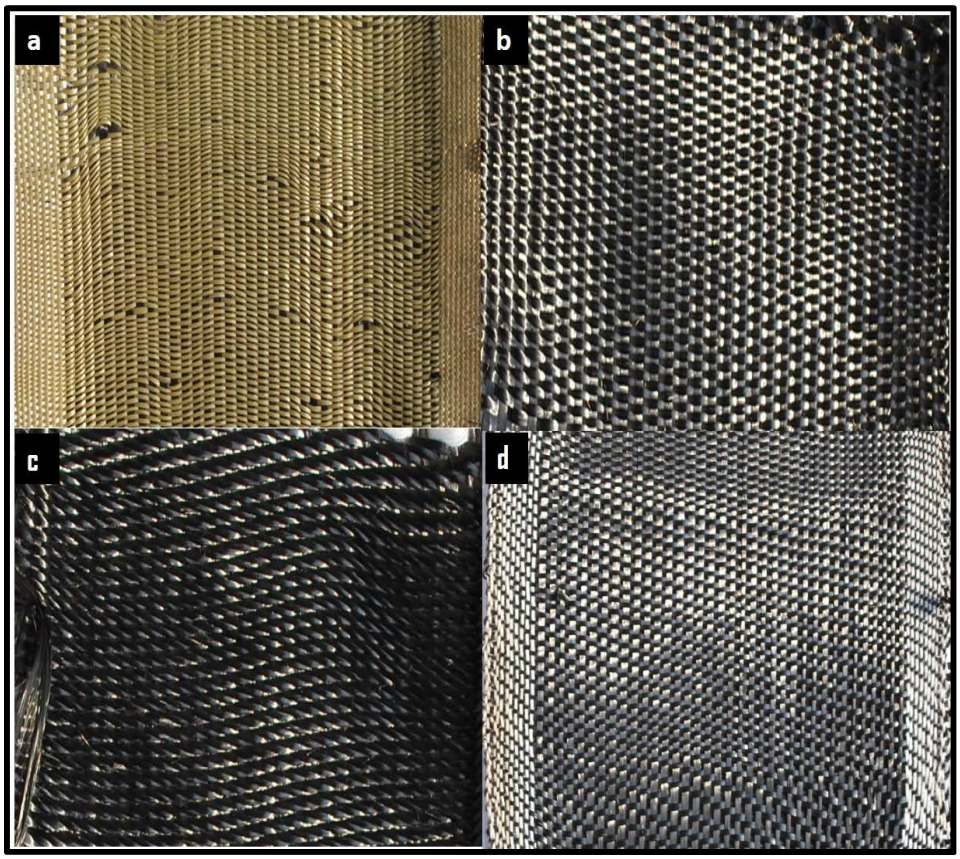

Figure 3.3: Typical image of initial samples prepared on handloom samples
[(a) *K* x *K* - Plain, (b) C_{6K} x C_{6K} - Plain, (c) C_{12K} x C_{12K} - Plain, (d) C_{6K} x C_{6K} - Twill]

Troubleshooting. Reed having count 12 and heald wire were cleaned mechanically and chemically to make it smooth before using them. To avoid problem like fraying and breakage paraffin wax was applied on yarn. But, after some trail it was found that applying wax on machine parts was more effective compared to applying it on the yarn.

B. Preparation of sample on power-loom

Carbon tow pirn was prepared on an ordinary pirn winding machine. Afterwards, while weaving on power-loom several problems such as improper unwinding, trapping of weft in the shuttle eye, inadequate working of the temple, misfunctioning of take-up mechanism were experienced.

Troubleshooting. Twisting of Carbon yarn was tried, to avoid improper unwinding and weft trapping in shuttle eye. But the results were not acceptable. Even after application of PVA adhesive the above problem persists.

Moreover, roller temple was unable to hold fabric. Trials of other temple like ring and ring roller could not deliver the desired performance. There was problem of slippage in conventional take-up mechanism. To avoid slippage extra spring load could not give satisfactory results. This led to slacking of fabric.

As a result, trials on power-loom were discontinued and switched on sample preparation on CCI sample loom.

C. Preparation of samples on CCI sample loom

Preparation of samples on CCI loom was divided into two parts:

1. Preparation of weaver's beam on CCI single end warping machine (Figure 3.4a). Description of the machine is given in Appendix-I.

2. Preparation of samples on CCI rigid rapier loom (Figure 3.4b). Description of the machine is given in Appendix-II.

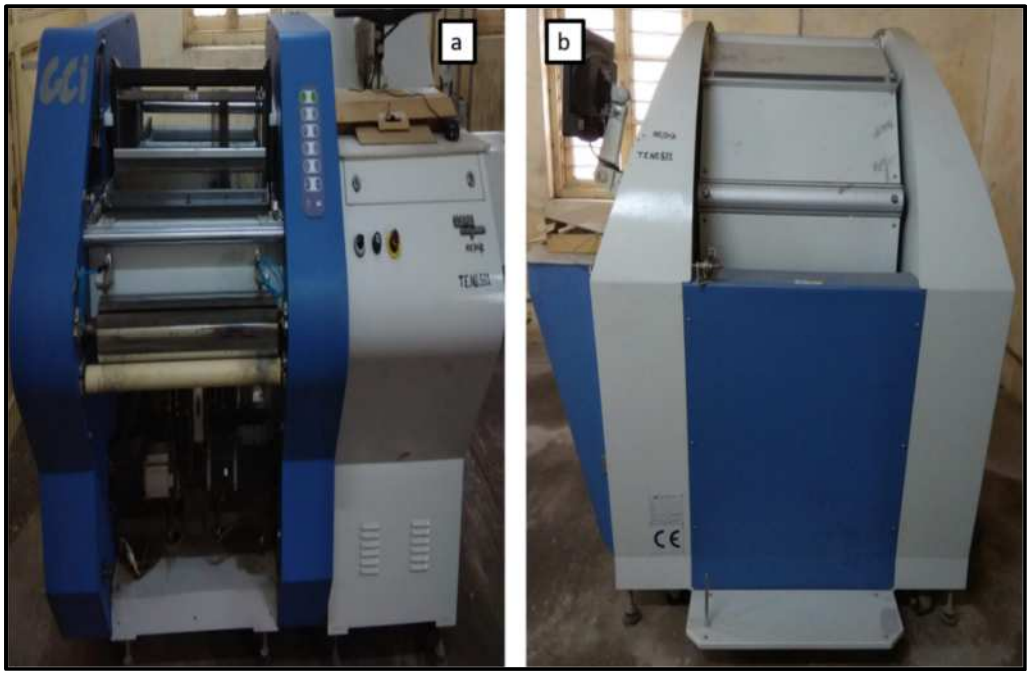

Figure 3.4: (a) CCI Rigid rapier loom and (b) CCI single end warping machine

Part 1.

A weaver's beam of width 20" was prepared using 6K Carbon tow on single end warping machine. There were two major problems incurred while trying to weave Carbon fibre on CCI single warping machine. First, the overhead withdrawal of yarn provided in the machine was inserting false twist during the warping process. Second, the round guides provided in the CCI machine was causing fraying of the Carbon tow.

Troubleshooting. By replacing overhead withdrawl system to sidedrawl of the package, the false twisting problem was resolved. There was no inbuilt arrangement to installing package for side withdrawal. To feed tow horizontally to warping machine, a special arrangement was made. Two inserts having same dimension as of inner diameter of spool was fixed on both the sides as shown in Figure 3.5. By installing this spool on a round rod it acted like double flanged bobbin. This gave a satisfactory withdrawl of tow without any false twisting. The problem of fraying of tow, mostly due to abrasion was solved by replacing existing circular guide with rectangular guide. This arrangement gave a satisfactory working of CCI warping machine and a proper set-up was prepared.

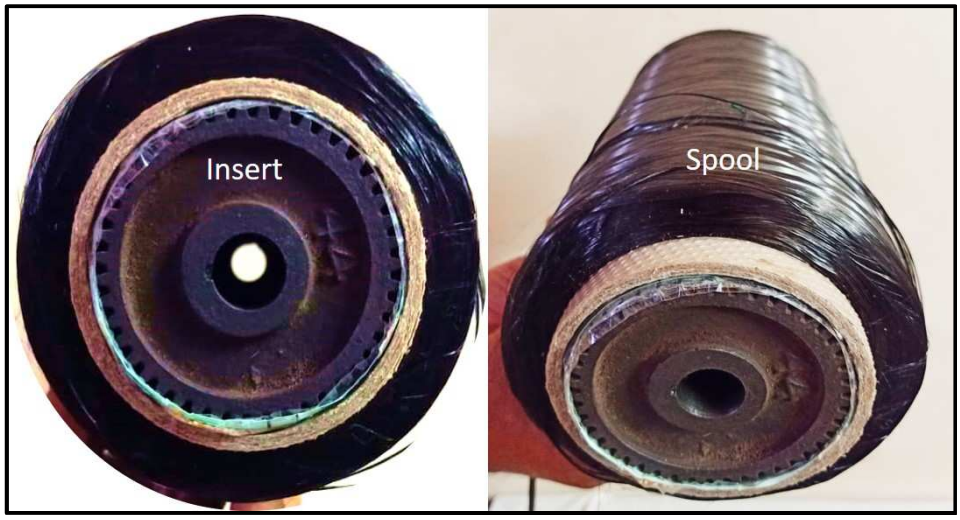

Figure 3.5: Arrangement on package for side withdrawal on CCI single end warping machine

Part 2.

The inherent features of the loom were not suitable to weave Carbon tow. For weaving Carbon yarn certain modification were made on CCI rigid rapier sample loom. The experience gained during weaving of sample on handloom and power loom gave the insight to make modification on the loom.

Leasing. Unusual difficulties were experienced while trying to weave Carbon fabric on this loom. A trial of glass lease rods for shedding motion did not work and continuous slippage and entanglement of Carbon tow was persisting. Then, the direct passage of Carbon tow was tried with which satisfactory operation. The figure of final set-up is shown in Figure 3.6.

Shedding. Another major modification was made is of heald wire. The original heald wire had a rectangular cross-section with sharp corner was causing high abrasion which led to breakage of the yarn.

Beating. For trouble free weaving, the existing reed was replaced by newly designed reed. The existing was having flat and sharp dents which was causing splitting of Carbon tow during beating. Hence, a newly designed reed was fabricated to resolve this splitting of Carbon tow issue.

Figure 3.6: Path of the warp at the back of the loom

Front rest. Existing front rest of the loom was leading to excessive abrasion of Carbon tow.

Take up. Existing take up path consist of three rollers which was giving excessive bending. This excess bending was causing improper and misaligned winding which resulted in distortion of the fabric.

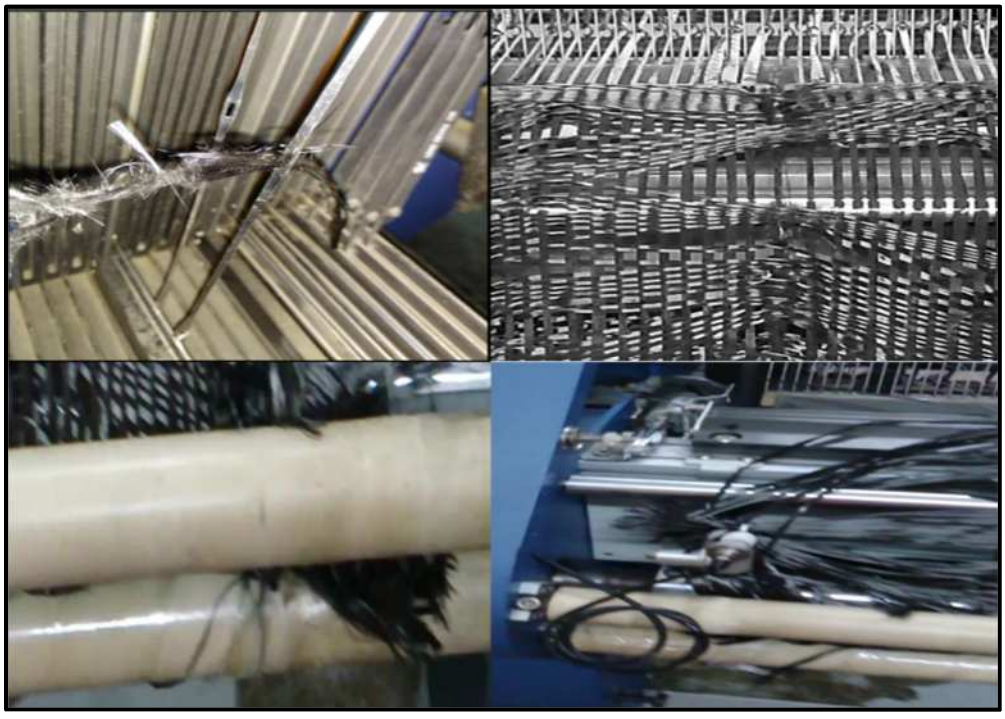

Figure 3.7: Damage to Carbon yarn during preliminary weaving

Weft passage. There was an excessive abrasion to the Carbon yarn due to guides and tensioner along weft passage. It was observed that these excess abrasions were due to excessive no. of guides present in the passage. The excessive were bypassed from the passage. Damages caused during motion to the Carbon tow are illustrated in Figure 3.7.

Troubleshooting. The major modifications made to weave Carbon tow trouble free are as follows:

Heald wire. Original inbuilt rectangular heald eye was modified and fabricated to oval shaped heald eye in the newly developed heald wire. The size oval eye was designed in such a way that there is no hindrance in free movement of the Carbon yarn. This modification prevented the breakage of the Carbon yarn due to abrasion. The newly developed heald wire as depicted in Figure 3.8 gave satisfactory outcome.

Reed. A new developed reed (Figure 3.9) was developed and fabricated. The reed count ‘50’ was replaced to ‘6’ to accommodate the width of the Carbon tow. In the new reed, a smooth polished rounded stainless-steel dent was used instead of existing flat sharp iron dent to reduce abrasion. The details of newly modified reeds are revealed in Figure 3.10. To accommodate the selvedge, a separate section of reed having count ‘25’ was used and attached to both sides of the reed. This selvedge arrangement gripped the weft yarn properly.

Front rest. Change in passage was adopted to avoid damage to fabric due to existing front rest. In the existing set up on loom fabric has to pass through two grooves with help of guide rods. This was causing unwanted extra resistance to the fabric passage. In the new arrangement a smooth curved plate made of aluminium sheet was provided (Figure 3.11).

Take-up. The original provided nip rollers were creating accumulation of the fabric. The trail was made for winding of the fabric by removing nip rollers. It gave encouraging results. This arrangement was giving proper, aligned and without distortion of the fabric.

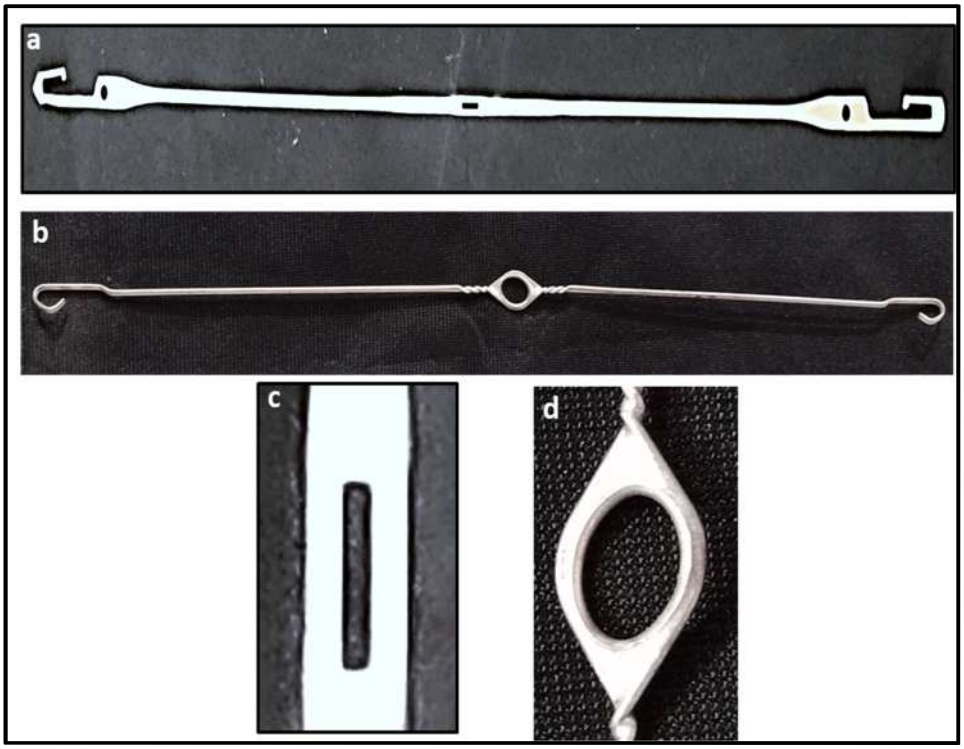

Figure 3.8: a) Original heald wire b) Modified heald wire c) Original heald eye and d) Modified heald eye

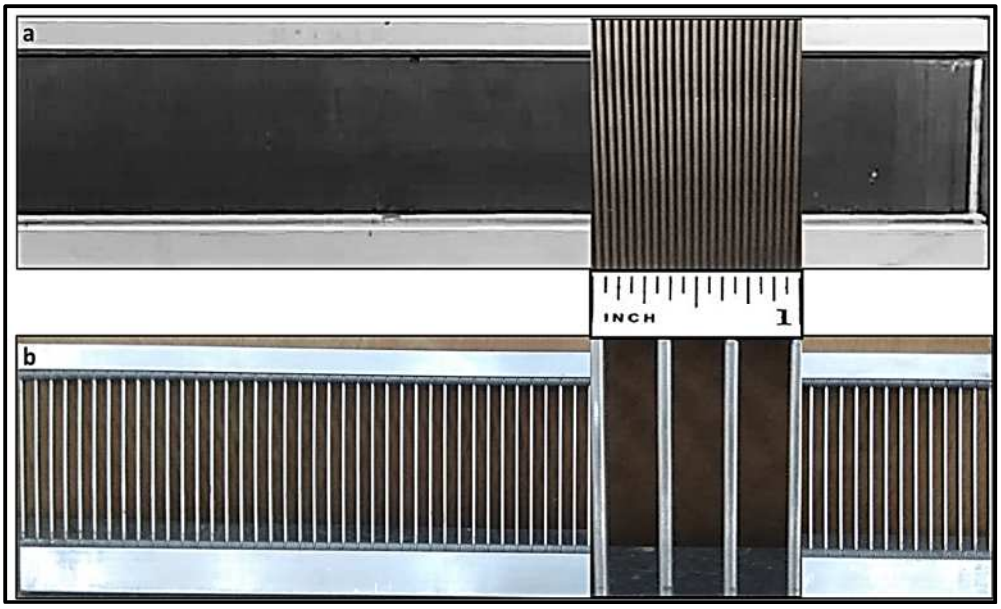

Figure 3.9: a) Original reed (reed count=25); Modified reed (reed count=6)

On this modified CCI sample loom, several hybrid fabrics by using 12K Carbon, 6K Carbon, Kevlar and HDPE were prepared. The summary of prepared fabrics is shown in Table 3.1.

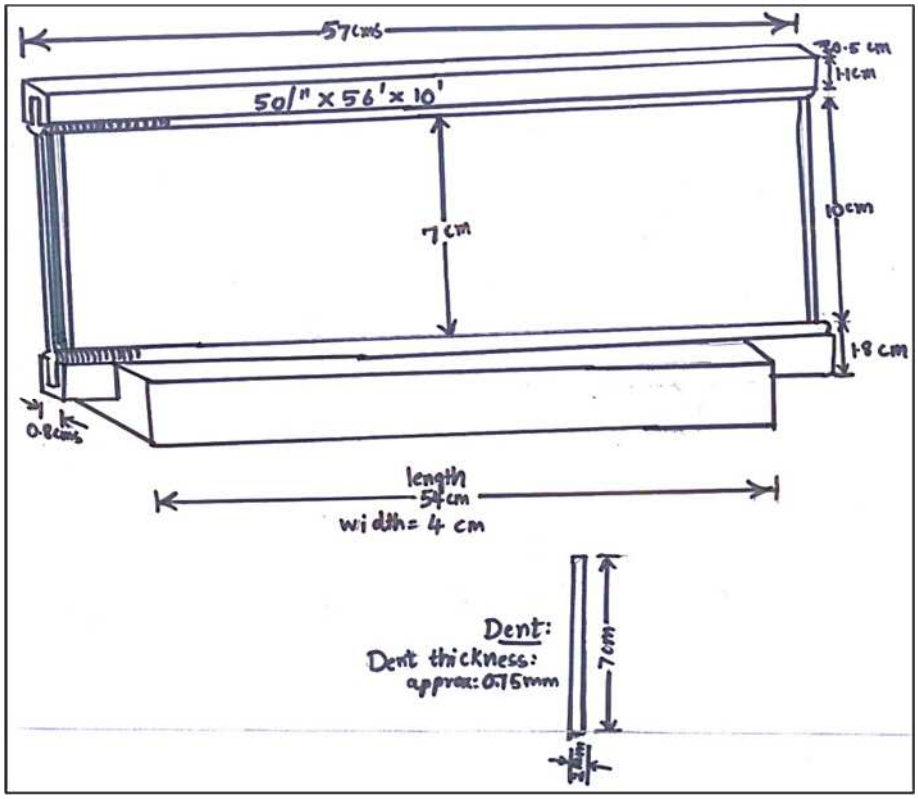

Figure 3.10: Schematic diagram of newly developed modified reed with dimensions

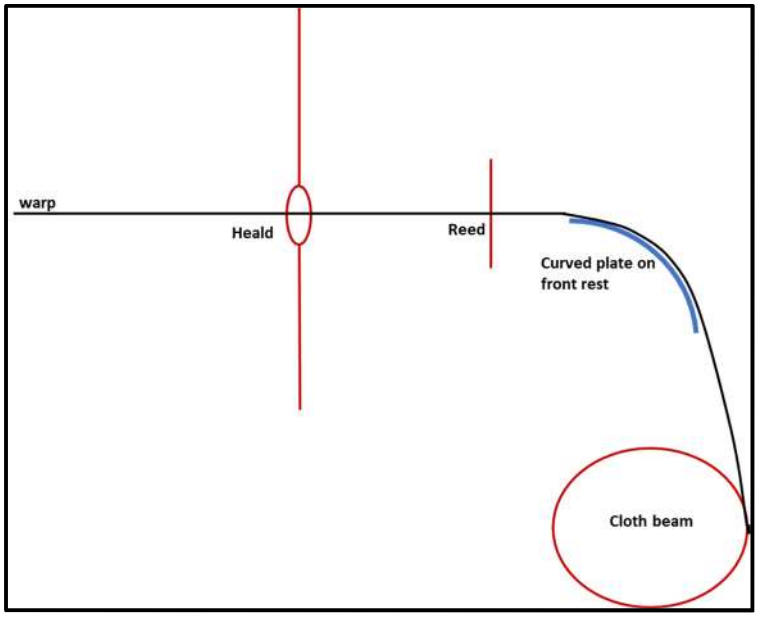

Figure 3.11: Schematic diagram modified arrangement for take-up on CCI loom

Table 3.1: Summary of fabrics prepared on modified CCI sample loom

Sr. No	Sample code	Warp	Weft	Weave	EPI	PPI	GSM	Thickness (cm)
1	$(C_{12K}C_{6K})_P$ Fig. 3.21a (1)	6K Carbon	12K Carbon	Plain	8	8	384.966	0.046
2	$(C_{12K}H)_P$ Fig. 3.21a (2)	HDPE	12K Carbon	Plain	12	12	399.55	0.050
3	$(C_{12K}H)_T$ Fig. 3.21a (3)	HDPE	12K Carbon	Twill	12	12	416.32	0.053
4	$(C_{12K}H)$ Fig. 3.21a (4)	HDPE	12K Carbon	Sateen	12	12	392.30	0.043
5	$(KH)_P$ Fig. 3.21a (5)	HDPE	Kevlar	Plain	12	18	259.04	0.052

C_{12K} - **12K Carbon;** C_{6K} **- 6K Carbon; K - Kevlar; P- Plain; T-Twill; S- Sateen**

Section II

3.3 Preparation of composite sample

For this work different composites samples were prepared from differently oriented textile fabrics by using hand lay-up technique. This type of composites is known as textile polymer composite laminates (PTCL).

3.3.1 Conjectural Trials

Initial trail started by considering epoxy resin based on epoxy-catalyst system. The sample was prepared having size, (length 300mm, width 300mm, thickness 40mm) die at reputed institution. The prepared sample was very flexible and at elevated temperature (60ºC) it was losing its strength, so further trial on this resin was discontinued. The sample is shown in Figure 3.12 (a and b)

Next trail was tried with different epoxy resin based on epoxy-hardener system. The pilot trial to assess the strength of this epoxy resin was done by making a small round sample which was cut to dumbbell shape (width=10mm and thickness=4mm) as shown Figure 3.13 (a and b). Its strength was tested.

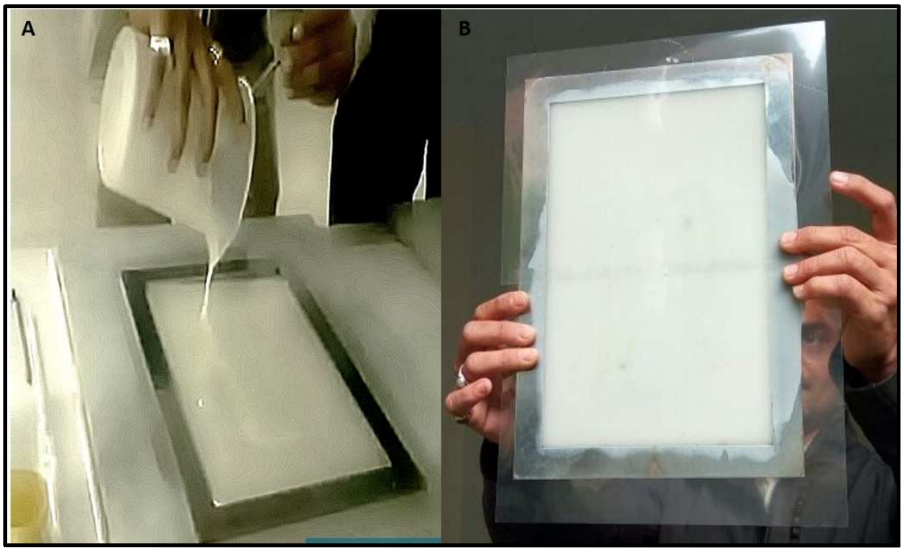

Figure 3.12: Initial matrix sheet preparation a) Preparation stage of matrix sheet b) Cured matrix sheet

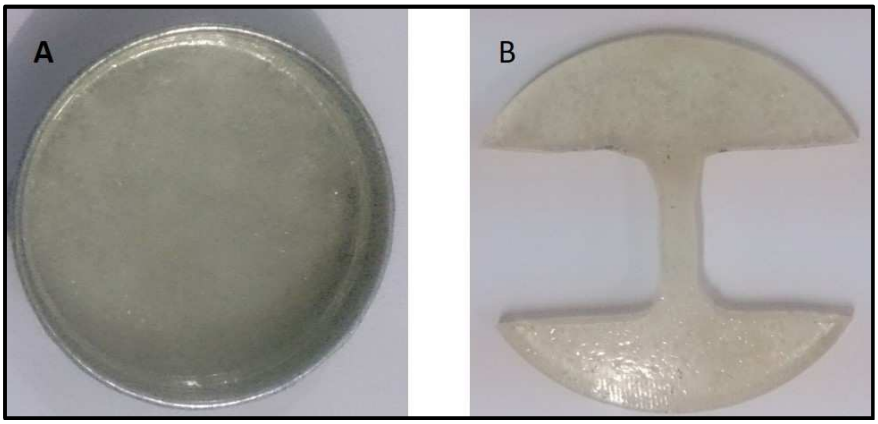

Figure 3.13: Initial preparation of matrix specimen. [a: polymer matrix cured in round shape; b: polymer matrix cut to dumbbell shape]

It gave 42 MPa tensile strength. Then single layer composite was prepared as shown in Figure 3.14. It was found that the prepared composite sample was sufficiently stiff, so trail with this system was further continued.

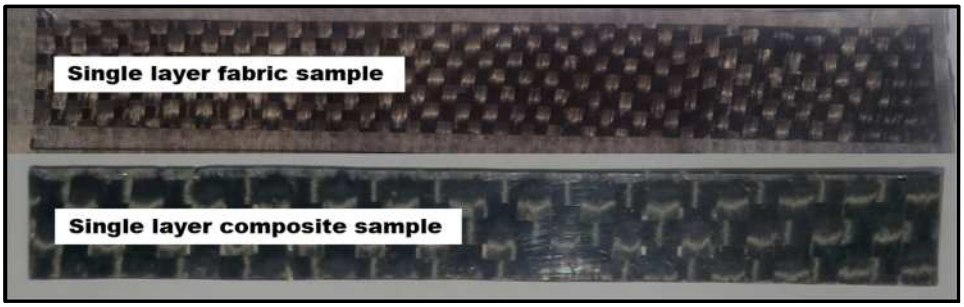

Figure 3.14: Single layer fabric composite sample

In third trial, three layered composites were prepared as shown in the Figure 3.15. Here, three set having fabric sequence: 0/0/0, 0/45/0 and 0/90/0 were prepared. The tensile strength of these samples was 235, 58.9 and 207 MPa respectively.

In these sequences middle layer was giving strength in one direction only i.e. 0/45/0. So, necessity of one extra layer in middle was envisaged. So that strength is uniformly distributed in the composite.

In next trial, four layered composites were prepared. here, a set having fabric sequence, 0/+45/-45/0, was prepared. In this sample tensile strength was obtained as 175.70 Mpa in longitudinal direction and 352.68 Mpa in transverse direction.

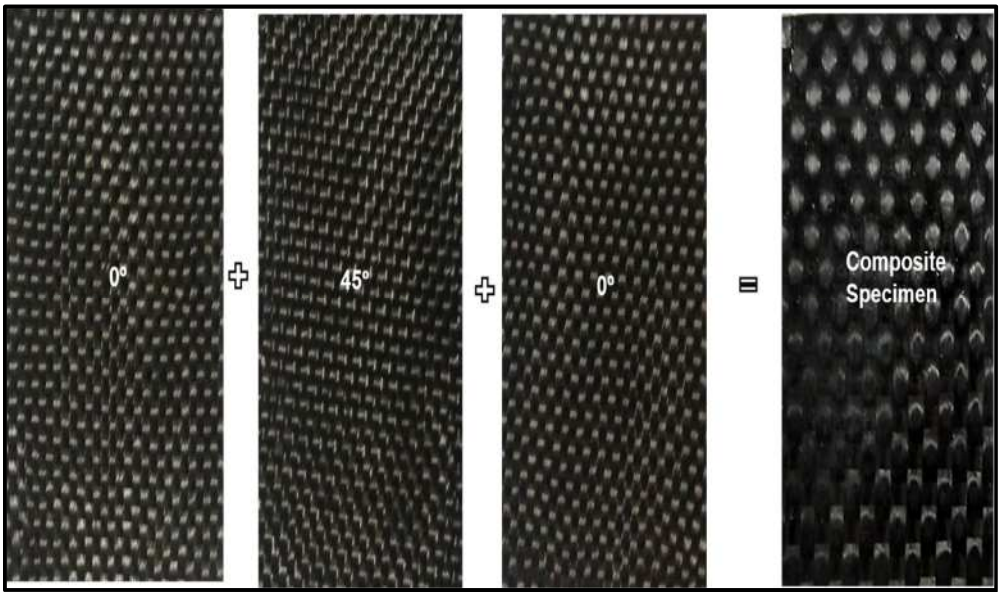

Figure 3.15: Three layered fabric composite sample

3.3.2 Preparation of appropriate fabric specimen for required composite

The fabric was woven on rigid rapier sample loom. The required fabric was chosen for reinforcement. Then the fabric sample of required dimension and at required angle (axis in the longitudinal direction) was marked by suitable marker. It was taken care to mark the angle of fabric accurately. Along, with angles 0° and 90°, care was taken to mark the skew angles ±30°, ±45° and ±60° properly. Schematic diagram of typical skew angle ±45° is shown in the Figure

3.16a. The adhesive tape was applied to prevent spreading out of fabric during and after cutting as shown in Figure 3.16b.

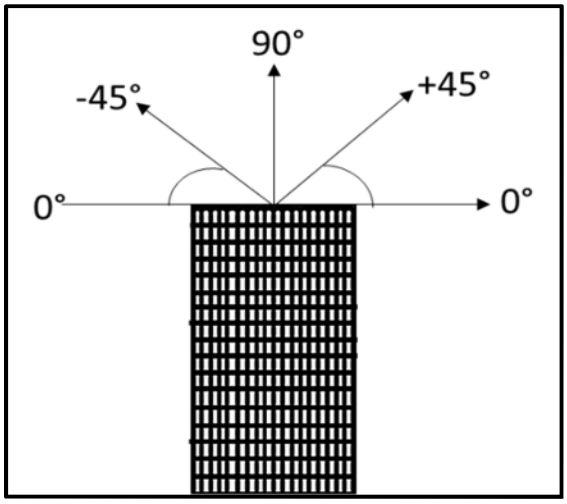

Figure 3.16a: Schematic diagram for skew angle (±45°) with respect to warp (0°)

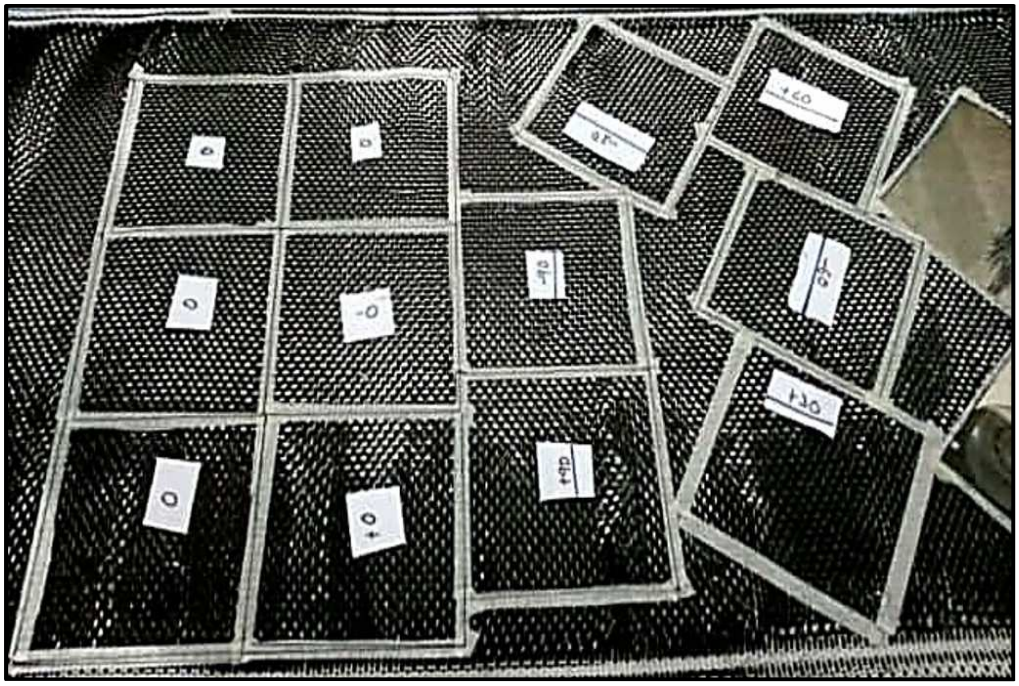

Figure 3.16b: Marking and labelling on fabric for cutting.

3.3.3 Preparation of matrix

To prepare proper matrix different chemicals are required viz. resin, catalyst, modifier. The required chemical in required quantities were cooled to 5° C in a refrigerator to avoid pot polymerisation of resin mix as explained in detail in

subsequent section (Figure 3.17d). When desired temperature was achieved then preparation of resin was started.

Firstly, required quantity of the resin (20% excess than theoretical) was weighed accurately on digital balance in disposable paper cup (Figure 3.17a). The required quantity was calculated by formula given in equation 3.1 as below:

$$W_r = weight\ of\ resin\ in\ g$$

$$= \frac{l\ x\ w\ x\ t\ x\ 1.2}{1000\ x\ \rho} \qquad (3.1)$$

Where,

l = length of the sample, mm

w = width of the sample, mm

t = thickness of the sample, mm

ρ = density of the sample, g/cc

Required quantity of initiator was poured accurately in resin (Figure 3.17b). Here, precaution was taken that no excess initiator is dropped. As once excess drop is mixed with resin it cannot be reverted, which compel to discard the mass and new sample to be prepared. This cause to loss of costly resin. The ratio of resin to initiator is kept as W_{resin}: $W_{initiator}$ = 10:1.5.

After weighing accurately, the resin and initiator in the same container, it was mixed thoroughly using wooden stick (Figure 3.17c). To avoid the air trapping in the mass, two drops of air releasing agent was added. By adding air releasing agent, the void formation in the final composite were reduced. Then, two drops of coupling agent were added to create a chemical bridge between the reinforcement and matrix. It improves the interfacial adhesion between the two phases. Again, in this formulation 1 ml of temperature stabiliser was added.

This polymerisation is exothermic and temperature sensitive hence after preparation this mass is kept in the refrigerator to maintain its temperature below 5° C. At room temperature the polymerisation gets initiated. As the polymerisation is exothermic the temperature of mass will start increasing. The exothermic heat raises the temperature. The polymer gets trapped into vicious circle. Higher the temperature higher the rate of polymerisation. This led to

complete pot polymerisation within 30 minutes. The pot polymerised mass is shown in Figure 3.17d.

Meanwhile, the set-up for composite preparation is initiated (Figure 3.18 (1-11)).

Figure 3.17: Resin preparation steps

Here, in this work epoxy resin thermoset matrix has been used. Epoxy resin formulations are typically providing as two separate parts which are mixed just prior to application.

The Material used was:

1. **Epoxy resins.** Functionalised Epoxy polymer resin grade Polysil 100EC. Liquid epoxy resin based on diglyceride ether bisphenol having different molecular weight ranging from (5x103 – 40x109) modified by silanolamine.

2. **Catalyst.** VT – 150C
3. **Coupling agent.** VT – 400CA
4. **Air releasing agent.** VT – 450ARA

The Equipment used for resin mix preparation were pipette, test tube, weighing scale, paper glass, candy sticks. The details about the functionalised epoxy polymer resin are stated in Table 3.2 as follows:

Table 3.2: Properties of functionalised epoxy polymer resin grade

Sr no	Parameter	Range	Observation
1	Appearance	Visual	Viscous liquid
2	Colour, visual	Colourless	Colourless
3	Density	1-1.1	1.02
4	Stabilizer, PPM (parts per million)	90-100	98
5	Anti-settling agent performance	No settling after centrifuge	No settling after centrifuge
6	Reactive monomer content % titration method	3-5%	4.8%
7	Unreacted ester content, titration method	Nil	Nil
8	Filer bonding agent, titration method	2-3%	2.5%

3.3.4 Fabrication of the textile polymer composite laminate (TPCL)

In this work, the study is confined to study the effect of orientation of fabric on the physical and mechanical properties of TPCL. for reliable results, preparation of a uniform quality of composite is necessary. To produce different samples of TPCL, the following standard preparation process is adopted.

Preparation of support and cover. In this work, for devoping polymer composite laminate smooth mirror polished granite stones were used for

supporting and covering the composite. The cleaned and dried supporting stone was kept on a flat table and levelled properly by using spirit level (bubble level) instrument along both the axes (Figure 3.18 b, c). This followed by placing PVC plastic film and applying a thin layer of mold release compound. Then, axes were marked accurately to keep sample in centre. Similarly, another granite stone having mirror polish surface was cleaned, dried and marked for the axes. A releasing agent was applied on PVC plastic sheet and kept ready.

Pressurizing weights preparation. To produce composite of consistent quality, the most important variable is compression of composite at constant pressure. To ensure uniform and constant load, a calculated dead weight was used. The constant pressure of 7 kPa is maintained throughout this work. Both axes of the pieces of all weight are marked accurately. Equation 3.2 was used to calculate the required weight.

$$Required\ weight\ W_p = \frac{l * w * p}{9806} \qquad (3.2)$$

Where,

W_p = total weight including covering stone required to generate pressure 'p'

l = length, mm

w = width, mm

p = required pressure, kPa (here, it is 7 KPa)

Preparation of the composite. It was confirmed before commencing the process of preparation of composite that pre-preparation like resin, fabric layers, dead weights and other accessories are in order.

On a sturdy table all requisites are kept ready (Figure 3.18a) including (1) Prepared resin mass at temperature below 5º C (2) All fabrics are arranged in a proper sequence as needed to be stacked. (3) The required dead weight was set. (4) Two covering PVC sheets marked with both axes. (5) Properly cleaned spreading roller were placed. (6) Properly cleaned brush was kept ready. (7) Sufficient releasing agent with cotton. (8) Properly cleaned supporting and covering stone was kept ready.

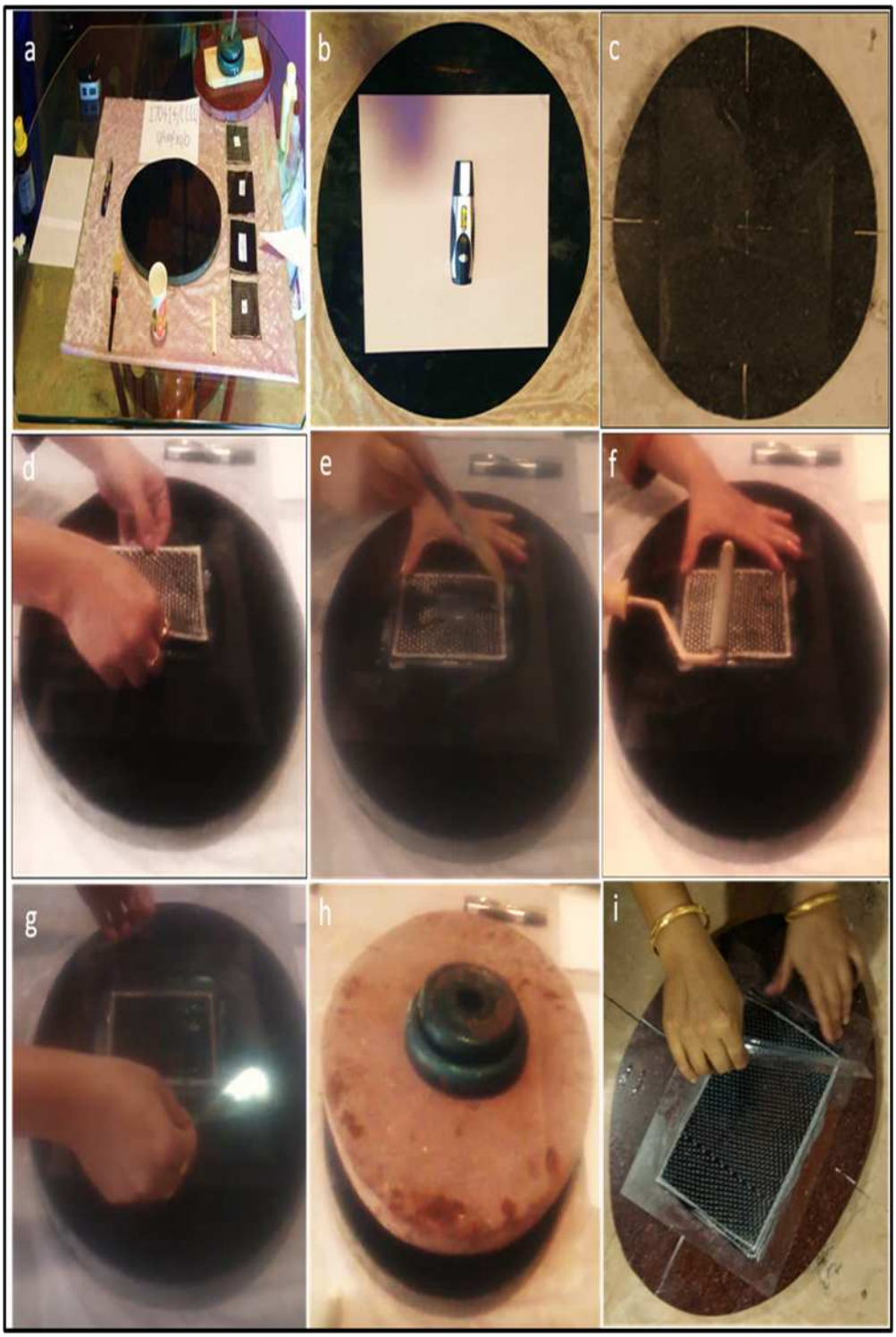

Figure 3.18: Sequence of polymer textile composite laminate.

After fixing releasing sheet aligned in both axes, a thin layer of releasing agent was applied. Then a thin layer of cooled resin was applied by brush uniformly. Next, first layer of fabric was placed over the resin layer ensuring alignment on both the axes (Figure 3.18d). After fixing first fabric layer a gently pressed hand

rolling is applied. This action will ensure the squeezing out of air bubble and uniform layer of resin.

After assuring that fabric is accurately fixed properly aligned, again a uniform thin layer of resin was applied by brush (Figure 3.18e). This follows fixing of second fabric layer. Here, it was ensured that fabric layer is kept at proper angle of orientation. After that the roller spreading is repeated (Figure 3.18f). This process of applying resin and fabric sequentially is continued till the required fabric layers four are completed.

Then the covering sheet with pre-coated releasing agent was put on the stack of fabric layers (Figure 3.18g). Finally, hand roller was applied and covered with covering stone ensuring alignment in both directions. Slowly apply the pre-weighted weights by matching their axes (Figure 3.18h). The sample was kept for two hours for curing. During this period all excess resin and air bubbles (Figure 3.19) were squeezed out. The composite sample covered with releasing plastic sheet was removed from both stones (Figure 3.18i).

Steps of preparation have been shown in Figure 3.18. Repetition of experiment was done. The above process is followed uniformly by preparing all the samples in this work. The detail of sequence and fabric are reported in Table 3.1

The schematic diagram of the setup of the hand layup method used in the composite preparation method has been given below Figure 3.20

Figure 3.19: Image showing air bubble squeezed out of composite

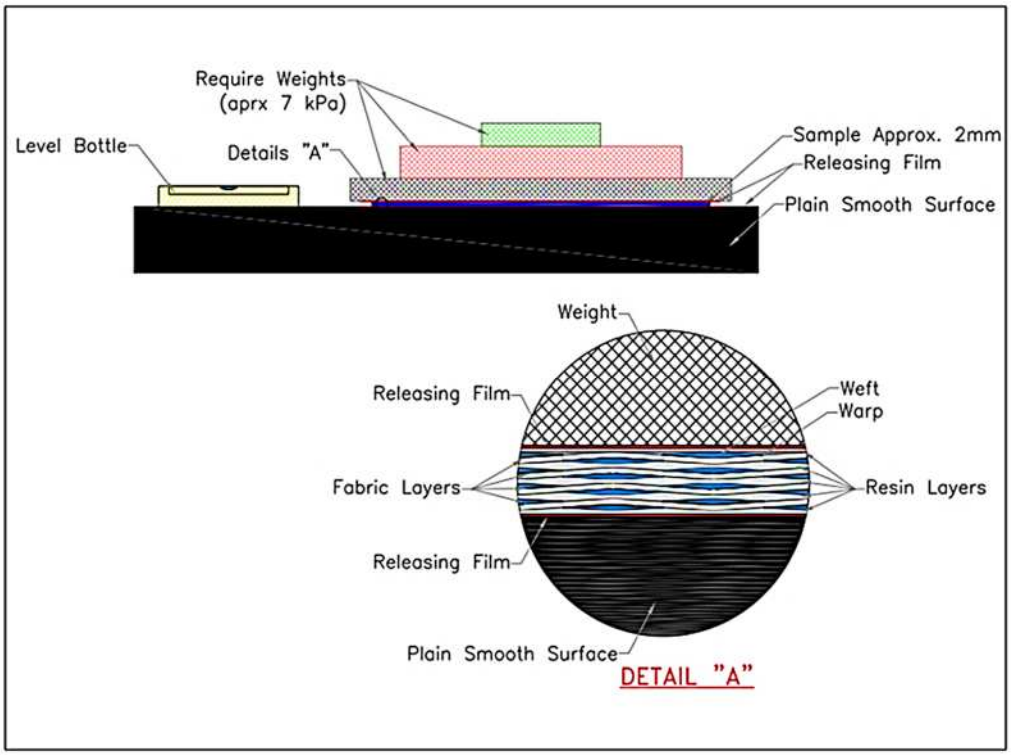

Figure 3.20: The hand lay-up set up

3.3.4.1 Laminate Stacking sequence

Hybrid composites offer a positive way of enhancing the mechanical properties like tensile, flexural and impact while it also helps to reduce the cost of engineering material. To improve impact properties of Carbon composites hybridisation with Kevlar was studied. Similarly, to reduce the cost of composite hybrid composite with HDPE were studied.

Constructing and designing with composites gives benefit of capability to contrast reinforcement material and orientation in a laminate with the help of plies. Loading on the laminate as a whole, as well as the out of plane (through thickness) loads that generate stress fields in each ply can be optimized.

To allow a suitable comparative analysis for each set, the number of plies for each material is kept constant. All the fabric samples prepared in this work as described in Table 3.1. The different composite samples as depicted in Table 3.3 are prepared and studied. Figure 3.21(b, c, d) shows schematic diagram of layering sequence of all the polymer textile composite laminates manufactured in this work.

Table 3.3: Details about the stacking sequences of TPCL.

Sample No.	Sample code	No. of layers	Laminate lay-up*	Type of laminate	Stacking sequence and orientation of fabric layers #
S1	CC1	4	[(0/0/0/0)]	Symmetric intraply	1st layer: $(C_{12K}C_{6K})_P$ at 0º 2nd layer: $(C_{12K}C_{6K})_P$ at 0º 3rd layer: $(C_{12K}C_{6K})_P$ at 0º 4th layer: $(C_{12K}C_{6K})_P$ at 0º
S2	CC2	4	[0/+30/-30/0]	Asymmetric intraply	1st layer: $(C_{12K}C_{6K})_P$ at 0º 2nd layer: $(C_{12K}C_{6K})_P$ at +30º 3rd layer: $(C_{12K}C_{6K})_P$ at -30º 4th layer: $(C_{12K}C_{6K})_P$ at 0º
S3	CC3	4	[0/+45/-45/0]	Asymmetric intraply	1st layer: $(C_{12K}C_{6K})_P$ at 0º 2nd layer: $(C_{12K}C_{6K})_P$ at +45º 3rd layer: $(C_{12K}C_{6K})_P$ at -45º 4th layer: $(C_{12K}C_{6K})_P$ at 0º
S4	CC4	4	[0/+60/-60/0]	Asymmetric intraply	1st layer: $(C_{12K}C_{6K})_P$ at 0º 2nd layer: $(C_{12K}C_{6K})_P$ at +60º 3rd layer: $(C_{12K}C_{6K})_P$ at -60º 4th layer: $(C_{12K}C_{6K})_P$ at 0º
S5	CC5	4	[0/+90/-90/0]	Asymmetric intraply	1st layer: $(C_{12K}C_{6K})_P$ at 0º 2nd layer: $(C_{12K}C_{6K})_P$ at +90º 3rd layer: $(C_{12K}C_{6K})_P$ at -90º 4th layer: $(C_{12K}C_{6K})_P$ at 0º
S6	CH1	4	[(0/0/0/0)]	Symmetric intraply	1st layer: $(C_{12K}H)_P$ at 0º 2nd layer: $(C_{12K}H)_P$ at 0º 3rd layer: $(C_{12K}H)_P$ at 0º 4th layer: $(C_{12K}H)_P$ at 0º
S7	CH2	4	[(0/0/0/0)]	Symmetric intraply	1st layer: $(C_{12K}H)_T$ at 0º 2nd layer: $(C_{12K}H)_T$ at 0º 3rd layer: $(C_{12K}H)_T$ at 0º 4th layer: $(C_{12K}H)_T$ at 0º
S8	CH3	4	[(0/0/0/0)]	Symmetric intraply	1st layer: $(C_{12K}H)_S$ at 0º 2nd layer: $(C_{12K}H)_S$ at 0º 3rd layer: $(C_{12K}H)_S$ at 0º 4th layer: $(C_{12K}H)_S$ at 0º
S9	KH1	4	[(0/0/0/0)]	Symmetric intraply	1st layer: $(KH)_P$ at 0º 2nd layer: $(KH)_P$ at 0º 3rd layer: $(KH)_P$ at 0º 4th layer: $(KH)_P$ at 0º
S10	CK	4	[(0/0/0/0)]	Symmetric intra-interply	1st layer: $(C_{12K}H)_P$ at 0º 2nd layer: $(KH)_P$ at 0º 3rd layer: $(KH)_P$ at 0º 4th layer: $(C_{12K}H)_P$ at 0º

For detail specifications of fabric layers refer Table 3.1

*stacking sequence – [(first layer/second layer/third layer/fourth layer)]

±30 indicate the warp yarn fibres in fabric are having 30º angle with standard normal fabric (with horizontal)

±45 indicate the warp yarn fibres in fabric are having 45º angle with standard normal fabric (with horizontal)

±60 indicate the warp yarn fibres in fabric are having 60º angle with standard normal fabric (with horizontal)

±90 indicate the warp yarn fibres in fabric are having 90º angle with standard normal fabric (with horizontal)

0 indicate the warp yarn in fabric are having 0º angle with horizontal

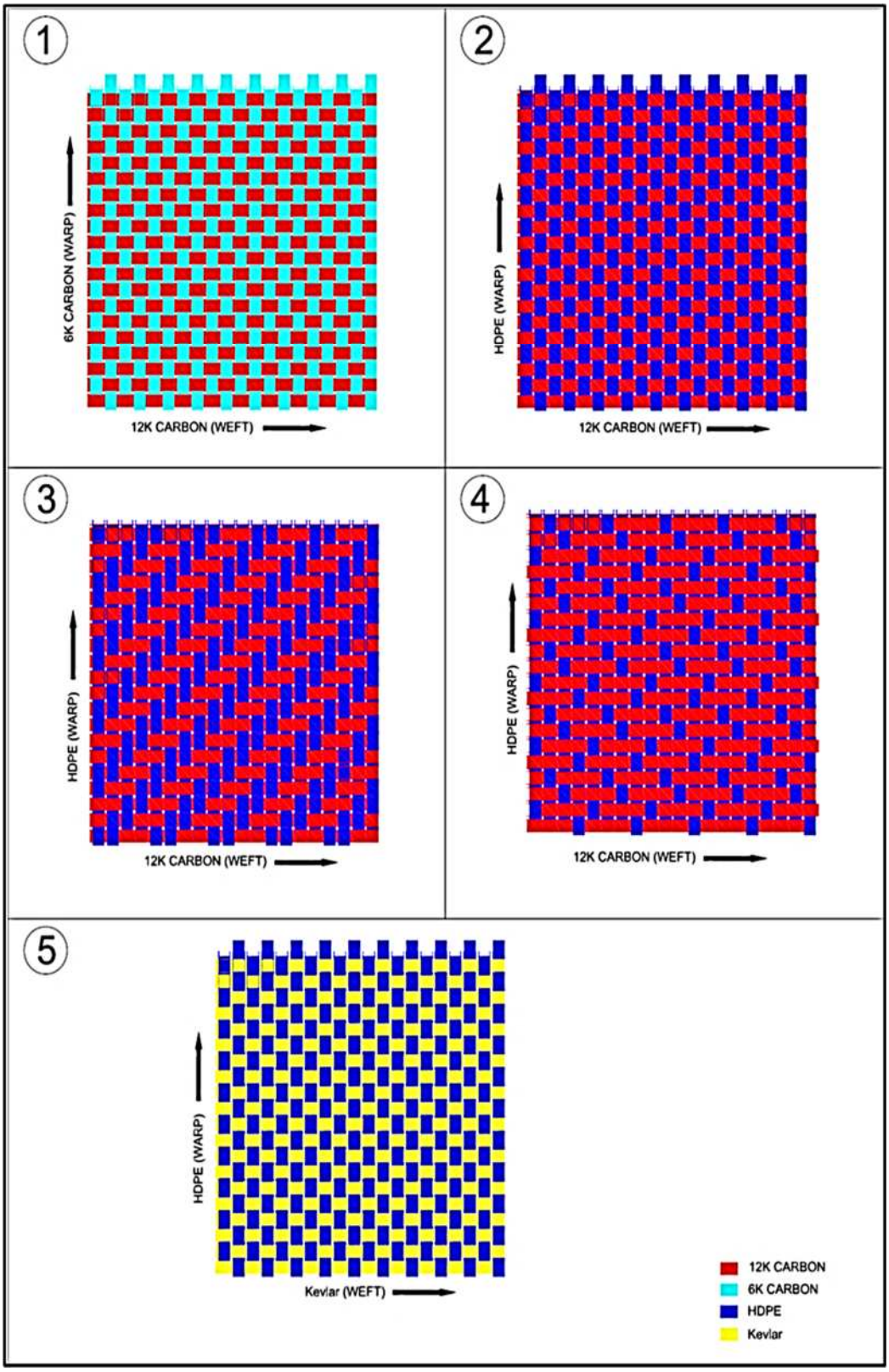

Figure 3.21a: Schematic diagram of fabric prepared
(1. $(C_{12K}C_{6K})_P$ 2. $(C_{12K}H)_P$ 3. $(C_{12K}H)_T$ 4. $(C_{12K}H)_S$ 5. $(KH)_P$)

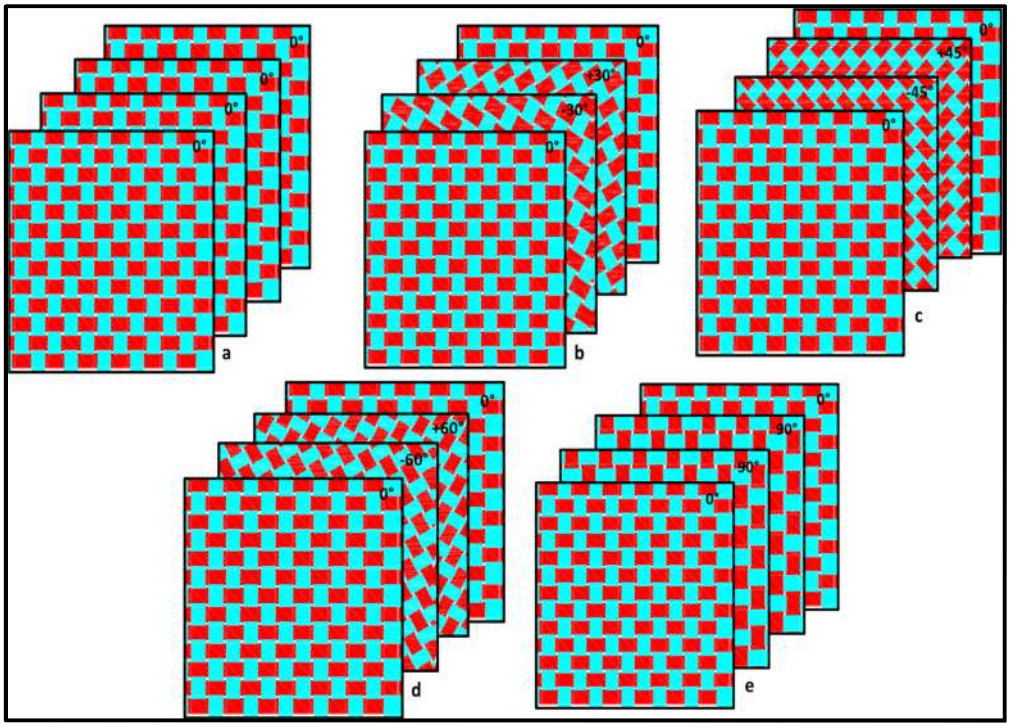

Figure 3.21b: Schematic diagram of layering sequence of Carbon-Carbon TPCL (a.CC1 b.CC2 c.CC3 d.CC4 e.CC5)

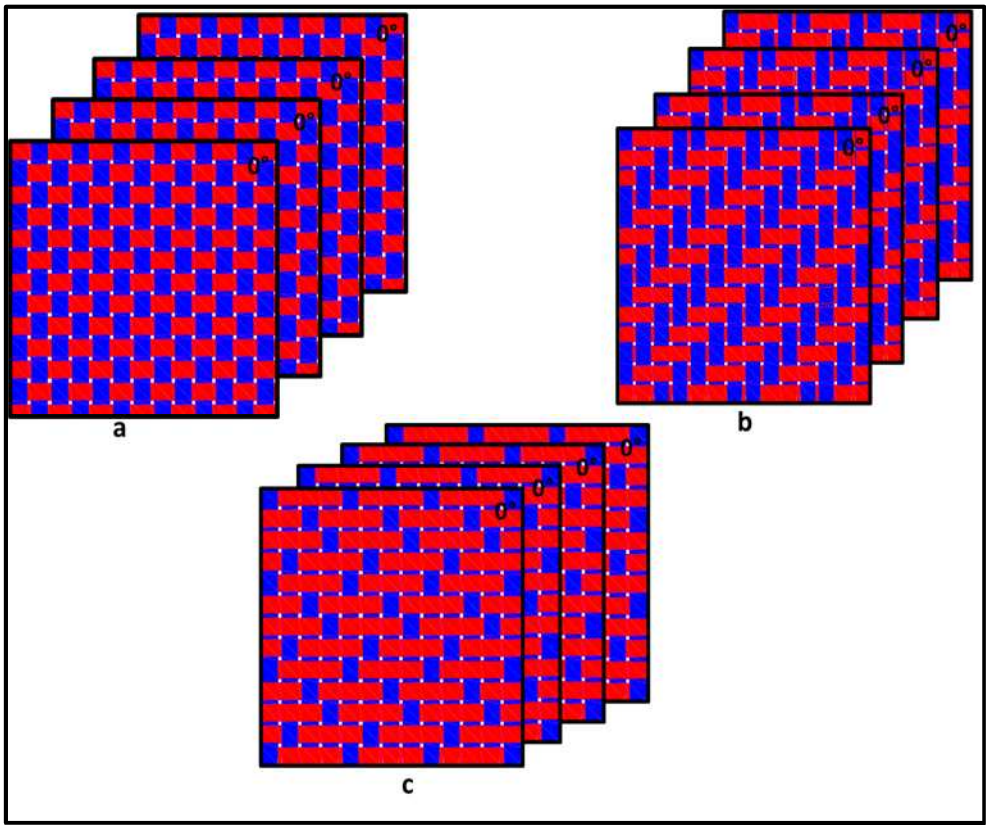

Figure 3.21c: Schematic diagram of layering sequence of Carbon-HDPE TPCL (a.CH1 b.CH2 c.CH3)

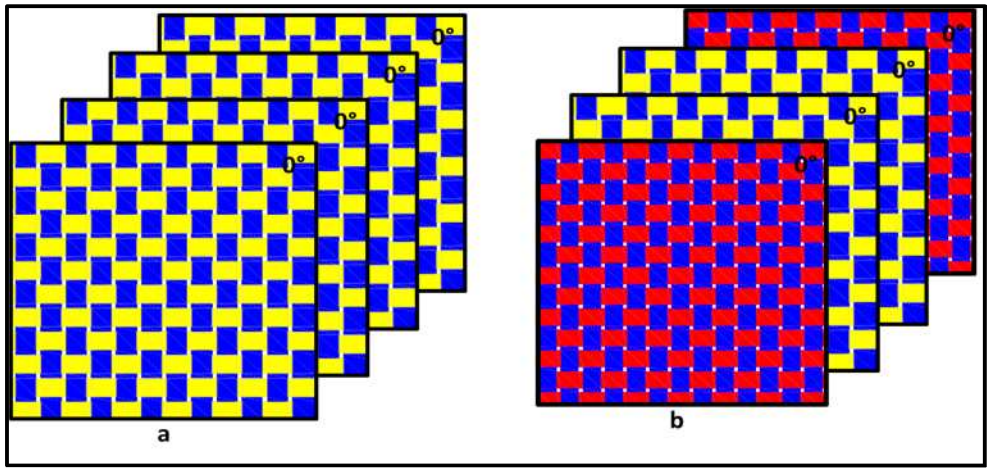

Figure 3.21d: Schematic diagram of layering sequence of Kevlar-Carbon-HDPE TPCL (a.KH1 and b.CK)

3.3.4.2 Preparation of specimen for testing

In this work, the composites were tested for their mechanical strength to compare the effect of fabric layer orientation, weave structure and reinforcement yarn. The different tests like tensile, flexural, impact and quasi indentation were performed. These all test require specific size of sample to perform the test.

Figure 3.22: Arrangement for cutting of composite samples

The composite is containing Carbon fibre. Carbon fibre cannot be cut by laser hence another technique is used to obtain proper size of sample. For this purpose, a high-speed cutter (6000 rpm, Hitachi having wheel size 4") is used. To have uniform width a template was prepared. Also, to avoid macro peeling the sample was fed slowly to the machine. Inhaling of Carbon fibre is injurious to health and also it has itching effect, hence operator worn full sleeves apron, glasses, safety mask, safety cap and gloves (Figure 3.22). Before the sample was cut proper marking was put in such a way that all cut samples possess it. After cutting samples were preserved properly.

Section III

3.4 Testing and Analysis.

In this work, composite specimens were prepared by using different fabric weaved from varied yarns namely 6K Carbon, 12K Carbon, Kevlar and HDPE. The basic properties of the yarns including their denier, density, number of filaments, tensile strength, strain and modulus of elasticity are depicted in the Table 3.4. Typical graphs showing tensile behaviour of the above-mentioned yarns are shown in Figure 3.23 (a-d)

Table 3.4: Basic physical properties of the reinforcement yarn.

Physical property	**12K Carbon**	**6KCarbon**	**Kevlar**	**HDPE**
Density (g/cm^3)	1.81	1.81	1.44	0.97
Linear density (Tex)	817	400	167.78	122
No. filaments	12000	6000	932	Flat
Tensile strength (g/tex)	92.4	99.98	175.09	53.01
Tensile strength (Mpa)*	1630	1764	2863	509
Strain %	2.64	1.63	6.49	19.82
Modulus of elasticity (Mpa)**	617.4	1082.0	595.4	25.7

*graphs are shown in Figure 3.22(a-d) ** calculated value

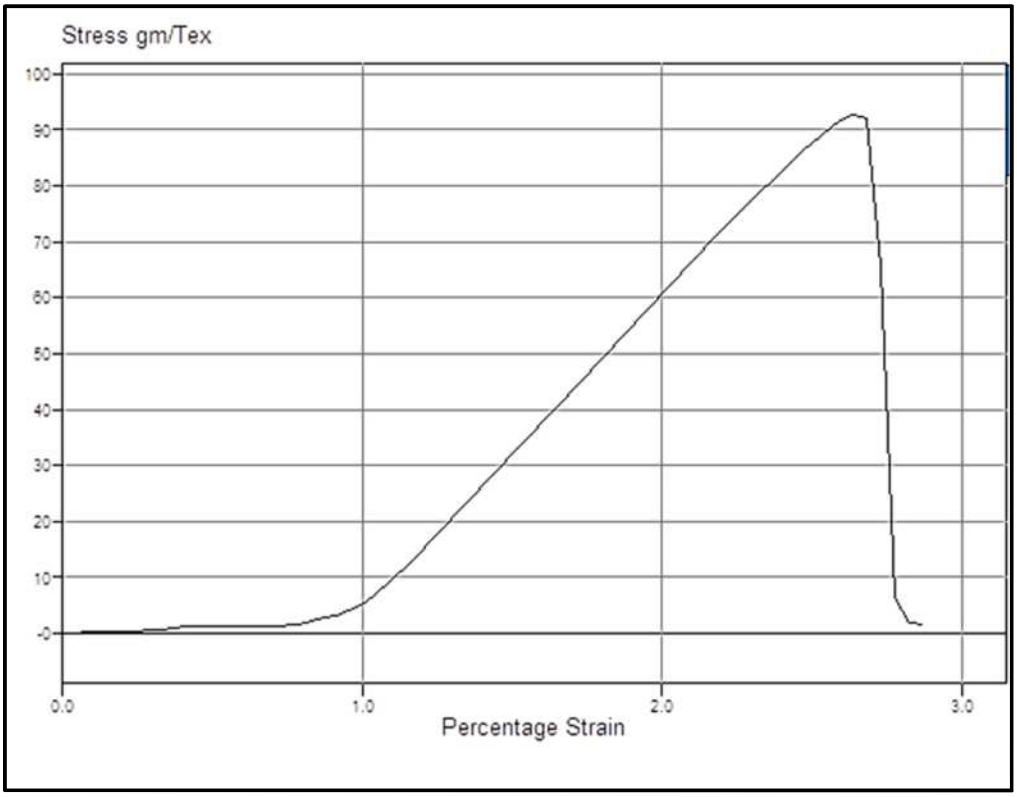

Figure 3.23a: Typical graph of stress v/s strain of 12K Carbon tow

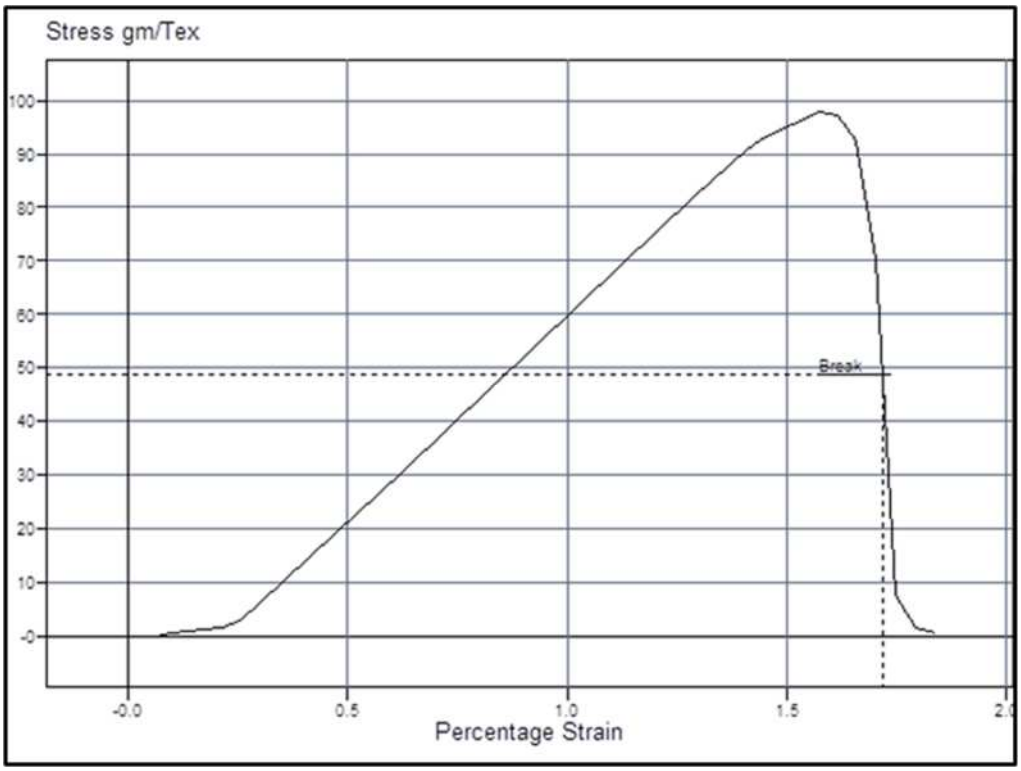

Figure 3.23b: Typical graph of stress v/s strain of 6K Carbon tow

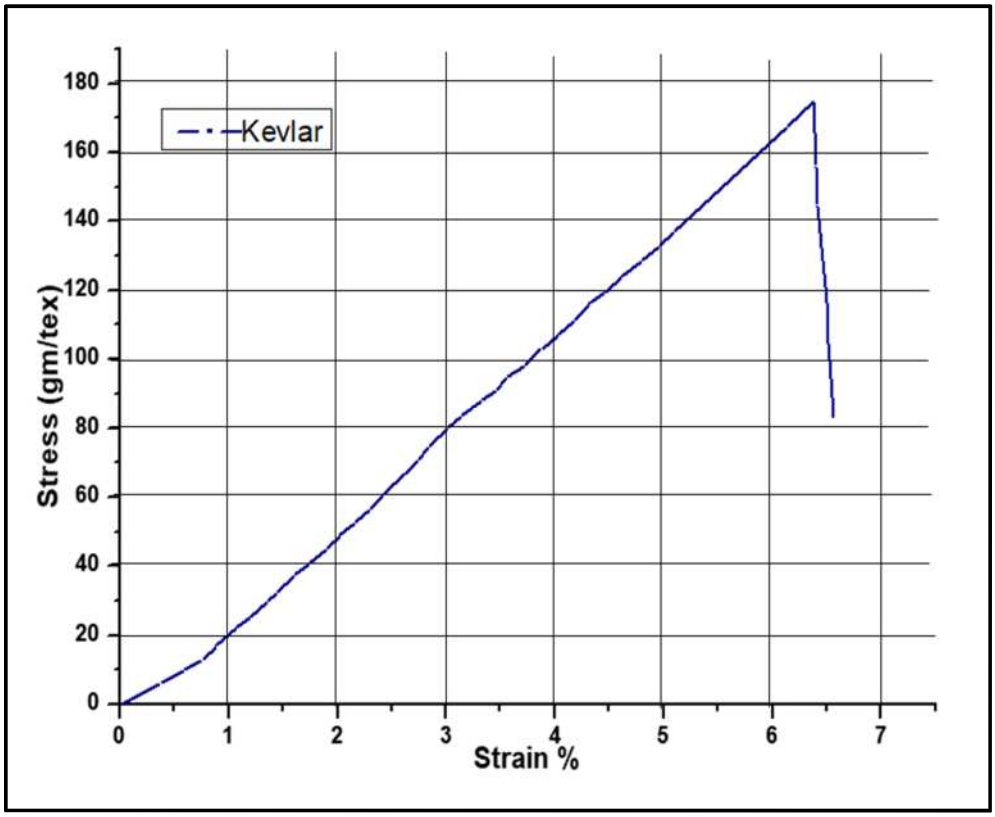

Figure 3.23c: Typical graph of stress v/s strain of Kevlar yarn

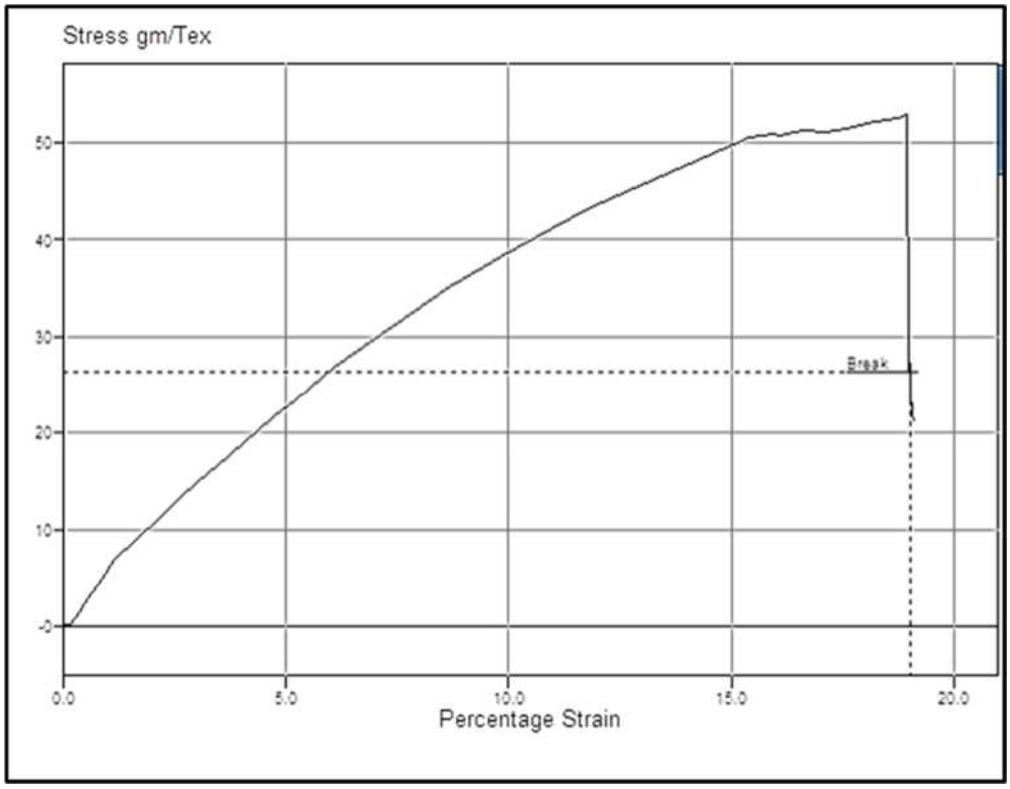

Figure 3.23d: Typical graph of stress v/s strain of HDPE yarn

3.4.1 Determination of physical properties of composites

The important physical properties: density, dimension measurement, fibre volume fraction is determined by using standard methods.

3.4.1.1 Dimensions measurement

Thickness of composite was determined by using a micrometre screw (Figure 3.23). Thickness at five different points of the sample was measured and averaged. The length and width of the composite samples were measured using a digital Vernier calliper at five different points and averaged. This methodology is used throughout the work wherever dimension measurement is required.

Figure 3.24: Dimension measurement of specimen

3.4.1.2 Density measurement

The density is measured by using Archimedes' principle. It states that for a body wholly or partially immersed in a fluid, the upward buoyant force acting on the body is equal to the weight of the fluid displaced by it [176].

Mass of the displaced liquid can also be expressed in terms of the density and

its volume. Further, density of an object is nothing but mass of object per unit volume. It is obvious that when an object wholly sinks in any liquid, it displaces an amount of liquid equal to its volume. If we apply Archimedes' principle in this situation, the buoyancy force on this sinked object is equal to the weight of the displaced liquid of the volume equal to the volume of the object. In the case of floating object, there is hundred percent weight loss. This implies that buoyancy force is equal to the weight of the object. Thus, when a body is partly or completely immersed in liquid:

$$\begin{aligned} \textit{Loss in weight of body} &= \textit{Weight of liquid displaced by the body} \\ &= \textit{Buoyant force or up thrust exerted by liquid on the body} \end{aligned} \qquad (3.3)$$

Accordingly, reduction in weight of an object is equal to the weight of the liquid displaced by it.

Considering a particular case of object sinking in liquid wholly but floating.

Rewriting equation 3.3:

$$\begin{aligned} \textit{Weight of body} &= \textit{Weight of liquid having volume equal to the object} \\ &= \textit{Buoyant force or up thrust exerted by liquid on the object} \end{aligned} \qquad (3.4)$$

In this work, to achieve this situation (i.e. the object is just sinked but still floating) [177] a procedure is being adopted. A liquid having high density (here, saturated solution of $CaCl_2$ solution) was poured in a glass container. Then a specimen was put in the solution. It was assured that it floats. Then, the water was added drop wise with continuous stirring till the specimen just sink wholly (Figure 3.24b). These liquids were labelled and preserved for further investigation. Same procedure is adopted for other samples (Figure 3.24 a, c). This is the situation as required i.e. object is sinked wholly but floating.

Now, as per Newton's second law,

$$W_s = weight\ of\ the\ sample = m_s . \frac{g}{g_c} \qquad (3.5)$$

Where,

m_s is mass of the object, kg

g is acceleration due to gravity m/sec^2

g_c is constant, kg./N.sec^2

Now,

$$density = \frac{mass}{volume} \quad i.e., \rho_s = \frac{m_s}{\mathrm{Vs}} \tag{3.6}$$

Substituting Equation 3.6 in 3.5

$$W_s = V_s \,.\rho_s \,.\frac{g}{g_c} \tag{3.7}$$

Similarly, Volume displaced by sample = V_s

$$\therefore \rho_l = \frac{m_l}{V_l} = \frac{W_l/(\frac{g}{g_c})}{V_l} \tag{3.8}$$

$$\therefore W_l = \rho_l \,.V_l.\frac{g}{g_c} \tag{3.9}$$

$$\therefore Weight\ of\ liquid\ displaced\ by\ sample = \rho_l \,.V_l.\frac{g}{g_c} \tag{3.10}$$

Now, at just sink position $V_l = V_s$ (3.11)

$$\therefore W_l = \rho_l \,.Vs.\frac{g}{g_c} \tag{3.12}$$

As per Archimedes principle,

$$W_s = W_l \tag{3.13}$$

$$\therefore V_s.\rho_s.\frac{g}{g_c} = V_l.\rho_l.\frac{g}{g_c} \tag{3.14}$$

$$\therefore \rho_s = \rho_l \tag{3.15}$$

Therefore, density of specimen is equal to density of liquid displaced. That indicate that at the situation i.e. the object (specimen) sinked wholly but floating: the density of sinked specimen and liquid are same.

After completing above experiment, the density of liquids is measured by specific gravity bottle method and are recorded in Appendix - III. The temperature during this whole procedure is kept constant at 30°C. This detailed process for measurement by specific gravity bottle in given in Appendix – III. Five specimens for each type of composite laminate were tested and average values were considered for further discussion.

$$Density\ of\ specimen\ \rho_s = sp.gr\ of\ liquid\ \times\ \rho_w \qquad (3.16)$$

Where,

ρ_w is density of water at same temperature

This method has an edge over commonly used other methods:

1) Weight is measured accurately on high accuracy balance, i.e. 1microgram
2) The accurate measurement of volume is not required, as the weight of water and liquid of constant volume (volume of specific gravity bottle) is measured

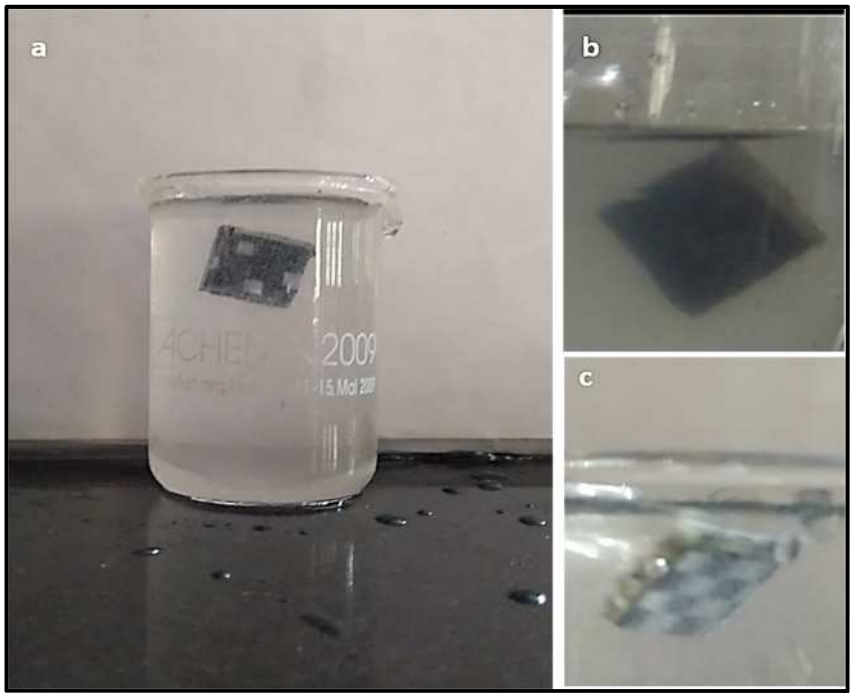

Figure 3.25: Density measurement

3) The errors in measuring dimension due to irregular shape is avoided.
4) The accurate density of water is known.

3.4.1.3 Fibre volume fraction

In this work, hybrid composite comprises of Carbon, Kevlar and HDPE as the reinforcing yarn. The use of burn out have limitations to estimate fibre volume fraction of the composite, which consist of Carbon and HDPE yarn. So, alternate method has to be developed to estimate fibre volume fraction. In a literature a theoretical method is proposed to determine fibre volume fraction for multiple layers of composite [178]. They developed an equation (2.6) which gives satisfactory results. In this work, we have adapted the same equation for developing a correlation to calculate fibre volume fraction. In their work, common fabric layers were used. Whereas, in this work intraply and interply hybrid composites are being studied (Table 3.2).

As discussed in Chapter 2, the equation 2.6 is rewritten as:

$$V_f = \frac{m.\alpha}{\rho.t_c} x \frac{1}{1000} \tag{3.17}$$

Where,

V_f = fibre volume fraction

m = fabric ply number in the composite

α = areal density of the fabric, g/m^2(GSM)

ρ = density of fibre, g/cm^3

t_c = thickness of composite, mm.

The above equation cannot be used for hybrid composites having different reinforcement yarn in layers. So, the equation is modified envisaging the intraply and interply hybrid composite so that each layer of the composite is taken into consideration and results are depicted in Appendix - IV.

The modified equation to consider for TPCL is written as follows:

$$V_f = \frac{m\sum\frac{\alpha_1}{\rho_o} + \frac{\alpha_2}{\rho_o} + \frac{\alpha_3}{\rho_o} + \_\_\_}{t_c} x \frac{1}{1000} \tag{3.18}$$

If all four layers are equal equation 3.18, can be modified as:

$$V_f = \frac{\frac{\alpha_1+\alpha_2+\alpha_3+\alpha_4}{\rho_o}}{t_c} x \frac{1}{1000} \quad (3.19)$$

$$\rho_o = \frac{d_1 n_1 + d_2 n_2}{w_1 t_1 n_1 + w_2 t_2 n_2} \quad (3.20)$$

Where,

V_f = fibre volume fraction

m = fabric ply number in the composite

α_1, α_2, α_3, α_4 = areal densities of 1st, 2nd, 3rd and 4th fabric layer, g/m^2(GSM)

t_c =thickness of composite, mm.

ρ_1, ρ_2, ρ_3…= densities of different fibres, g/cm^3.

ρ_o= average density of different fibres, g/cm^3

d_1, d_2 = weight per unit length, g/m

n_1 = ends per inch

n_2 = picks per inch

w_1, w_2 = width of tow/yarn, mm

t_1, t_2 = thickness of tow/yarn, mm

3.4.2 Mechanical properties

Ideally, all testing should be conducted using standardized test methods. The standardized test procedures described have been established by the American Society for Testing and Materials (ASTM, 100 Barr Harbour Drive, West Conshohocken, PA 19428-2959) and the Suppliers of Advanced Composite Materials Association (SACMA, 1600 Wilson Blvd., Suite 1008, Arlington, VA 22209).

The tests are intended for use with prepreg materials. While testing woven hybrid laminate, it's often necessary to modify the standardized test methods and consider other specialized methods as well. The individual tests have been established for specific purposes and applications. The mechanical response of textile composite laminates is dependent on the fibre architecture. Due to the interlacement and interweaving of the yarn in the fabric structure non uniform local displacement fields develop within the textile laminates, even under uniform axial extension. This characteristic is visible in unidirectional tape

materials laminates. Therefore, specimen and loading methods developed for tape type composites may not be applicable to textile composites according to Masters and Portanova, 1996, NASA [179]. These researchers have also mentioned in their report that textile composites are anisotropic in nature as compared to the tape prepregs composites. Consequently, standard composite testing methods may not be adequate to characterize these materials. This inhomogeneity may cause variability in the test results if done according to tape prepregs.

Mechanical characteristics include the determination of in-plane tensile, flexural, Izod impact test with notch and quasi-static indentation test. The mechanical properties of composites were investigated to study the effect of orientation, weave structure and reinforcement yarn on it. The composites were prepared by hand lay-up techniques having uniform epoxy resin and production conditions. To determine these properties ASTM D3039, D790 and D256 are referred [180-182]. Generally, rectangular specimens are required for the composite material characterization, because the “dog-bone” type tends to split in the region where the width changes as claimed by researcher (Jane et al., 2006). In this work, it was used rectangular specimens of TPCL composites in accordance to ASTM D3039.

3.4.2.1 Tensile properties

Tensile properties of samples (Table 3.2) were determined. Tensile tests were performed on Universal Testing Machine: TINIUS OLSEN/L-Series H50KL, capacity 5000 kg (Appendix V) (Figure 3.26 a-b).

Five specimens for each type of composite laminate were tested. Uniaxial tensile tests were conducted at 5.0 mm/min cross head travel (CHT). For uniformity the gauge length was kept same, 60mm, for all samples. The experiment was performed at temperature range of 25±2 ºC. Before starting the experiment all parameters of the specimen like length, width, thickness, CHT are fed in the dialog box of software. Then, loading was started. Then, it was assured that UTM is recording load v/s elongation graph. Load is continued till sample fails. This UTM machine automatically stops recording reading at its

failure. This is the end of experiment. Load v/s elongation recorded by machine was obtained for further study. Typical load v/s elongation are shown in Figure 3.27(a & b). The analysis is discussed in Chapter 4.

Figure 3.26a: Universal Testing Machine by TINIUS OLSEN/L-Series H50KL (Left); Sample fixture (Right)

Calculation of Ultimate tensile strength and modulus of elasticity (young's modulus).

The correlation obtained between load vs elongation by UTM are analyzed and arithmetically average value of elongation for the load are calculated for all the polymer laminated composite. These values of load vs elongation are used to calculate stress-strain correlation as per equation 3.21 and 3.22.

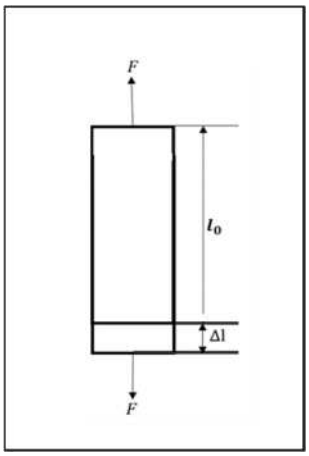

Figure 3.26b: Schematic diagram of tensile test

Young's modulus (E) is a measure of tensile elasticity, or the tendency of an object to deform along an axis when opposing forces are applied along that axis. It can be determined as the ratio of tensile stress to tensile strain at that point or it is the slope of the tangent of stress v/s strain graph at that point. Sometimes, it is referred as simply as the modulus of elasticity. It can be said that it is a tendency of deformation against opposite forces, which are applied to a particular axis.

To calculate the different parameters related to tensile strength following equations were used was used:

$$\text{stress} = \sigma = \frac{\text{load}}{\text{area}} = \frac{\text{F}}{\text{A}} \tag{3.21}$$

$$\text{strain} = \varepsilon = \frac{\text{change in length}}{\text{original length}} = \frac{\text{elongation}}{\text{original length}} = \frac{\Delta \text{l}}{\text{l}_0} \tag{3.22}$$

$$\%\ \text{elongation} = \frac{\text{change in length}}{\text{original length}} \times 10 = \frac{\text{elongation}}{\text{original length}} \times 100$$

$$= \frac{\Delta \text{l}}{\text{l}_0} \text{x} 100 \tag{3.23}$$

$$\text{Young Modulus} = \text{E} = \frac{\text{stress}}{\text{strain}} = \frac{\sigma}{\varepsilon} \tag{3.24}$$

Where,

σ = stress = tensile strength, MPa

ε = strain

F =load, N

A = average cross-sectional area, m^2

E=Young's modulus= modulus of elasticity, GPa

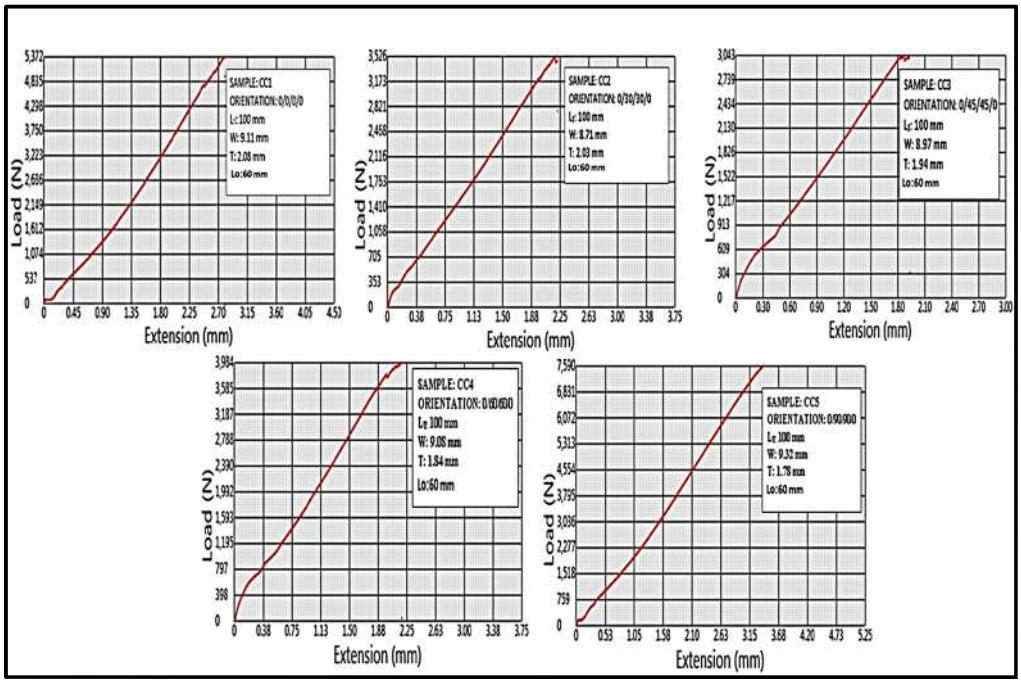

Figure 3.27 a: Typical graphs Load vs Extension (Elongation) for carbon-carbon composite in longitudinal direction for tensile property

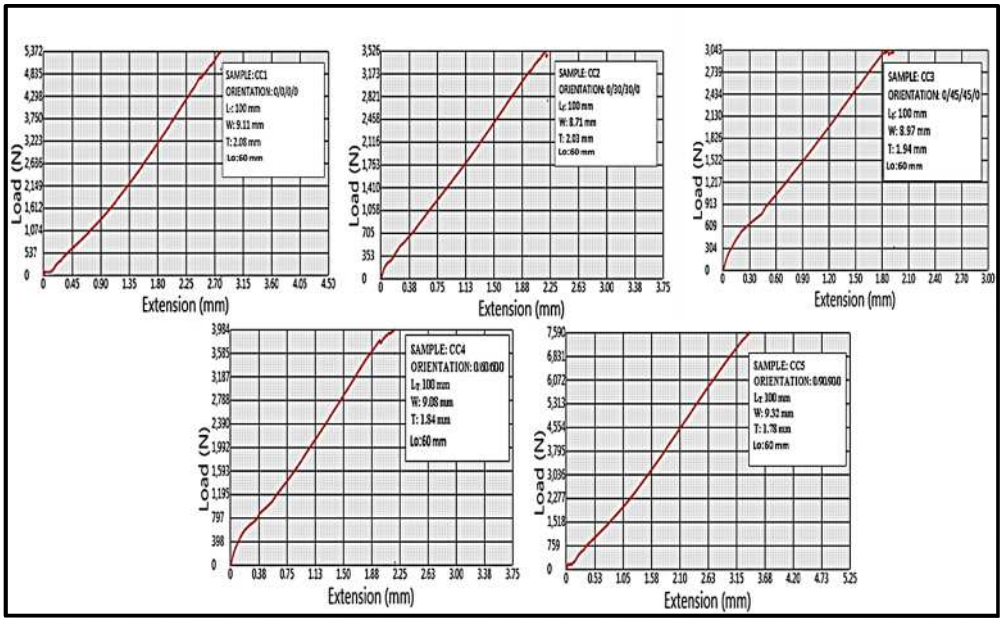

Figure 3.27 b: Typical graphs Load vs Extension (Elongation) for carbon-carbon composite in Transverse direction for tensile property

3.4.2.2 Flexural properties

The three-point bending test is the most common type for studying flexural properties. In this experiment flexural strength was tested on Universal Mechanical Testing Machine (shown in the Figure 3.30): FSA, max capacity 30KN, Model M-30 (FG-13/1) (Appendix VI) (Flexural test was conducted 1.3 mm/min at cross head travel (CHT) and hold time was taken as 1 sec. For uniformity the span length was maintained 50 mm. The experiment was performed at temperature range of 25±2 ºC.

Before starting the experiment all parameters of the specimen like length, width, thickness and CHT were fed in the dialog box (Figure 3.31) of software. The testing procedure involves placing the specimen in UTM and applying force to it until it fractures and breaks.

Loading was started and applied at the centre of two supports. Then, it was assured that UTM is recording load v/s elongation graph. Load is continued till sample failed. This UTM machine continues recording reading even after failure and till load reached zero. This was the end of experiment. Load v/s elongation recorded by machine was obtained for further study. The analysis is discussed in Chapter 4.

Calculation of flexural Strength and flexural modulus. The flexural strength is another important mechanical property to be considered for selecting proper engineering material. Flexural strength is the amount of force an object can take without breaking or permanently deforming when one tries to bend it. Practically, flexural strength tells us the maximum amount of stress (force the material can take per unit area in square meters or square inches).

The correlation obtained between load vs crosshead travel by UTM, as discussed below are analyzed. The average values of load and deformations are utilized to calculate stress v/s strain correlation for all the polymer textile laminated composite. For a three-point test, the flexural strength (given the symbol σ) can be calculated using:

$$\sigma_f = \frac{3FL}{2wh^2} \qquad (3.25)$$

$$E_B = \frac{L^3}{4wh^3} \times \frac{F}{m} \quad (3.26)$$

$$E_f = \frac{6mh}{L^2} \quad (3.27)$$

Where,

F= maximum force applied, Newton

L=span of the sample between the support, meter

w=width of the sample, meter

h = thickness of the sample, meter

σ_f =flexural strength, Newtons per meter square (Pa)

E_B= flexural modulus, Newtons per meter square (Pa)

m= the maximum displacement of center of specimen maximum force, meter

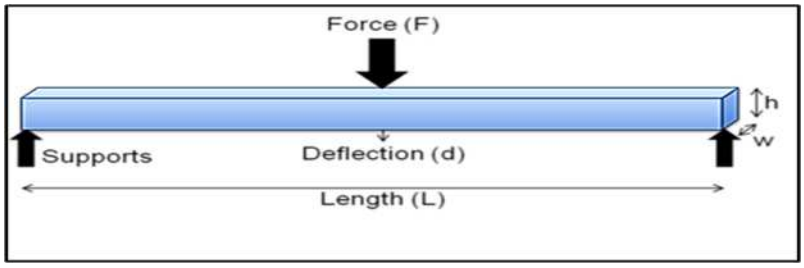

Figure 3.28: Schematic diagram of flexural test

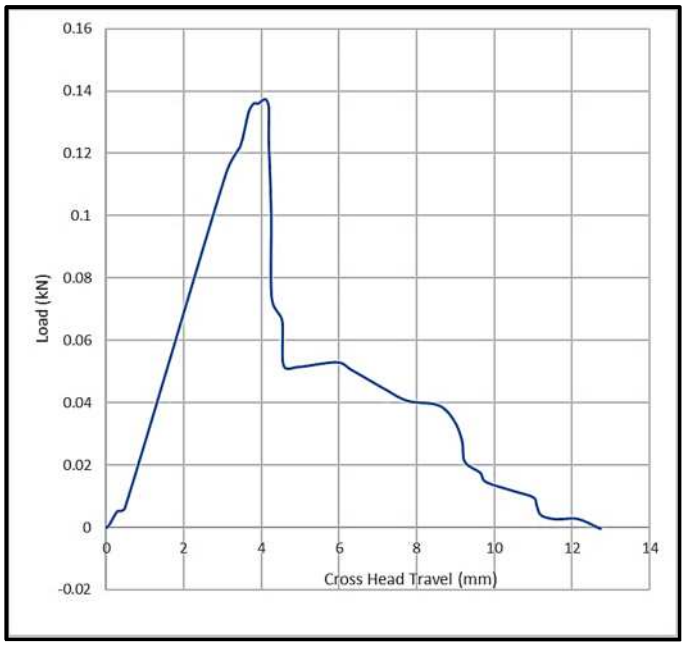

Figure 3.29: Typical graphs Load vs Cross head travel composite for flexural property

Figure 3.30: FSA Model M-30 (FG-13/1) UTM (Left); Sample Fixture (Right).

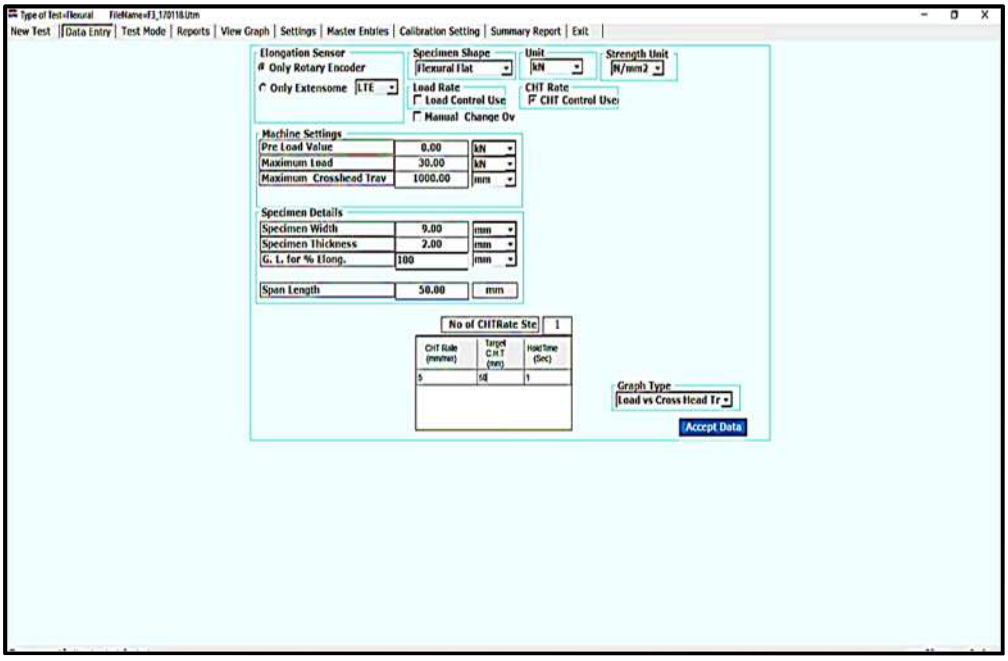

Figure 3.31: Dialog box of flexural test

3.4.2.3 Impact properties

Toughness is the most critical mechanical property of engineering material, as it influences the service life of the part. Common impact tests include Charpy, Izod, Dart Impact etc. Izod impact test is used to study the impact test in this work.

Izod impact test measures a materials resistance to impact from a swinging pendulum. Izod impact is defined as the kinetic energy needed to initiate the fracture and continue the fracture until the specimen breaks. Izod specimens are notched to prevent the deformation of specimen during impact. This test is used for quality check and comparison of materials for general toughness.

In this work XJUD-5.5 IZOD Impact Tester (Figure 3.32a) was used. For Notching purpose JJANM- 21 (Figure 3.32b) Notching Machine was used. After the test impact tester gives the absorbed energy in terms of joules.

For testing all dimensions of the specimen (length, width and thickness) were measured accurately and recorded. The sample was notched by using notching machine (Figure 3.32b). Sample was fixed in vice properly. The machine has maximum energy absorption up to 2.75J. Initially, before experiment starts impact tester shows energy absorbed as zero. Then, lever was operated to release the pendulum. This broke the sample. The energy absorbed by the

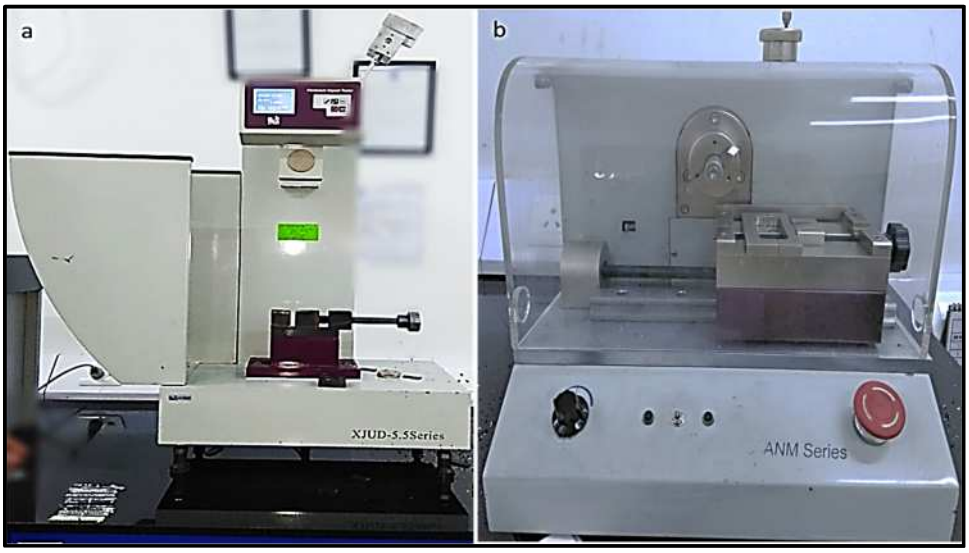

Figure 3.32: a) XJUD-5.5 IZOD Impact Tester. b) JJANM- 21 Notching machine.

sample to break it was displayed on the window. Reading were recorded and used for further studies. Three specimens of each composite were tested. The recorded readings are analysed in Chapter 4.

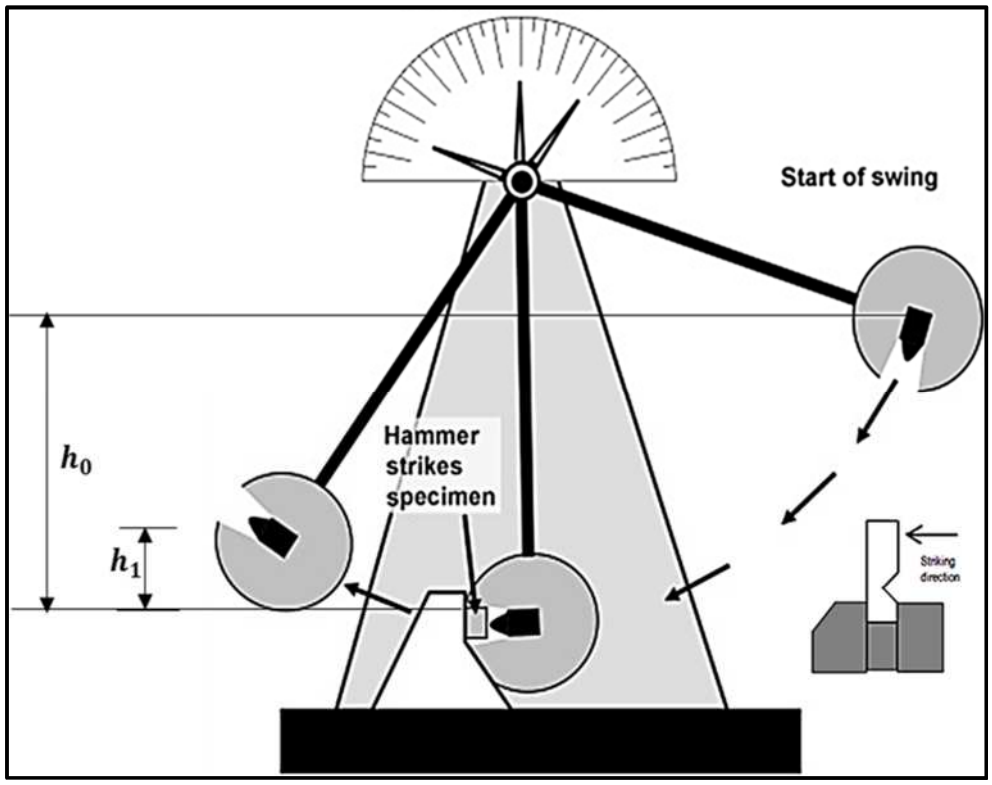

Figure 3.33: Schematic diagram of Izod impact test

Calculation of Impact Strength. Izod impact test measures the absorbed energy. The absorbed energy is the difference between energy applied and energy retained by the pendulum after impact that indicates energy required to rupture this specimen. Impact strength is expressed in kJ/m^2. Impact strength is calculated by dividing impact energy in J by the effective area under the notch. Some of the authors had named this absorbed energy as 'Impact toughness' or 'Impact energy'.

As depicted in Figure 3.33, in Izod impact test impact load which is produced by swinging of an impact weight from initial height (h_o). After releasing the pendulum, it strikes the sample and fractures the specimen at notch. After damaging the sample pendulum gain another height i.e. (h_1). The absorbed energy used for specimen fracture (U) is calculated as follows considering negligible frictional losses:

$$\text{Absorbed energy} = \text{intial potential energy} - \text{final potential energy}$$

$$U = m.g.h_0 - m.g.h_1 \quad (3.28)$$

$$U = m.\frac{g}{g_c}(h_o - h_1) \quad (3.29)$$

$$E_i = \frac{U}{A} = \frac{U}{w.t} \quad (3.30)$$

where,

U= absorbed energy, J

m= mass of the pendulum,

g = gravitational constant,

g_c= kg. m/N.sec^2

E_i = Impact strength, kJ/m^2

w = width of the specimen, m

t= thickness of the specimen, m

3.4.2.4 Damage resistance properties

As discussed in chapter 2, damage resistance is an important property to be considered while composite structures to be used as engineering material. In this work, the quasi-static indentation test was used to assess damage resistance. Quasi-static indentation tests are also known as static puncture test.

These tests are used to determine the puncture or rupture characteristics of a material. This is generally a compressive test where a material is compressed by an indenter or other type of device until the material ruptures or an elongation limit is achieved. In this method resistance of material to penetration of an indenter at a single constant speed, is determined under standard conditions. The test imparts a biaxial stress that is similar to the type of stress encountered in many product end user applications.

Research studies on quasi static indentation test have revealed that if support conditions are maintained, damage produced are comparable [127-128]. They further declared, when the maximum force applied during indentation testing is the same as the peak force produced during drop-weight impacting.

A universal testing machine, Instron (capacity 1000 kg) is utilized for this test. To accomplish this test, a special clamping device and indenter for the specimen was developed. The test specimen is clamped between two plates specifically designed for this test (Figure 3.34). The force is exerted at the centre of the specimen by an indenter (inset of the Figure 3.34). The experimental set-up of the quasi static indentation test along with all its newly developed parts have been shown in the Figure (3.34-3.36)

Detail of indenter and plunger developed for this work

A modified indenter was designed and fabricated from Ebonite (EN-24) material with the dimensions as given in Figure 3.33. The indenter was attached to the Instron UTM by means of a plunger onto the load cell. The plunger (Figure 3.34-3.36) was specially fabricated with required dimension to accommodate the indenter. Precaution was taken that the newly developed plunger does not damage load cell. Shape and size of tip of indenter was kept as similar to bullet (Figure 3.34;3.36). This was done, envisaging some further work which can correlate data from this quasi static indentation test with ballistic impact test.

Newly fabricated fixture and stand

A special stand was developed. The height of stand was kept enough so that it covers the fixture of the original UTM machine. This safeguard the original fixture of UTM. Two sufficiently strong matching discs were fabricated to hold the sample in the centre. A sufficiently wide hole, 16mm, is drilled in both the matching disc. The surrounded surface of the hole was made rough so that sample does not slip during the load application. Dimension details are given in Figure 3.36.

Experimental process

The specimens were marked and cut into the size 20x20 mm accurately by high speed cutting machine. The edges are cleaned by emery paper to make them smooth. The centre was marked on the specimen with the help of a marker. Then specimen was sandwiched between newly developed clamping matching disc.

After assuring proper tightening, these clamping discs are affixed on UTI machine.

The indenter was properly fit in the plunger on crosshead at upper side. The speed of crosshead was kept constant throughout the work. Then load was

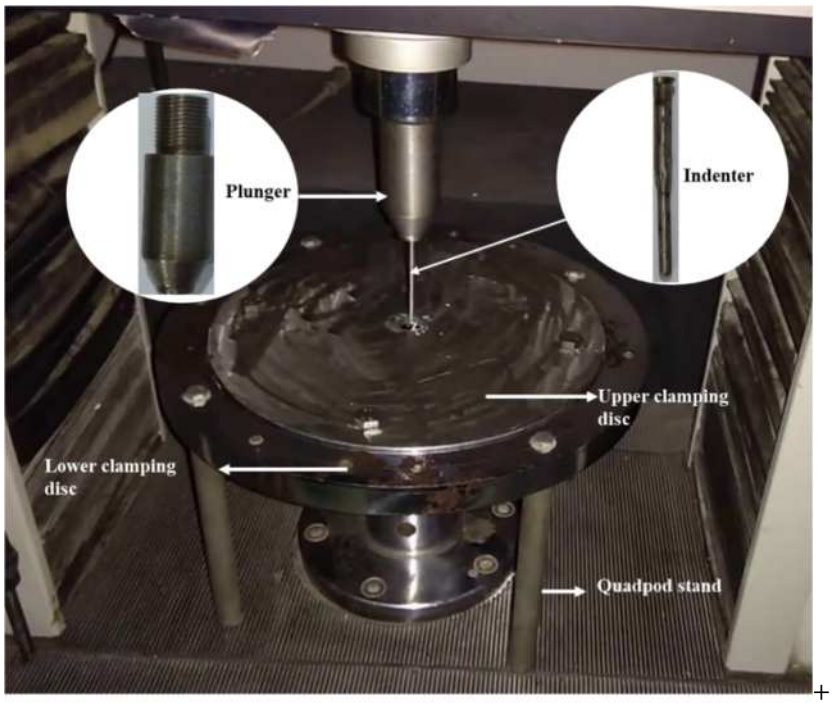

Figure 3.34: Quasi static indentation test set-up

applied. As indent starts moving with set speed. The software provided by the UTM machine starts recording the load vs displacement graph.

At certain load sample fails and graph of load v/s displacement drops down sharply. This was the end of experiment. Process was repeated for all other samples. The results are recorded and analysed in Chapter 4.

Calculation of Damage resistance Strength

This research work is basically to study the effect of orientation on different properties to compare damage resistance of different TPCL. A specific value 'σ′' is determined which is N/mm rather than commonly used N/mm^2. These results were also compared by calculating strength 'σ′' as determined by using equation 3.34. The detailed derivation is as per:

$$stress = \frac{F}{A} \quad (3.31)$$

$$\sigma_d = \left(\frac{F}{2\pi r b}\right) \quad (3.32)$$

Here, 2πr is constant

$$\therefore \sigma_d = \frac{KF}{b} \quad (3.33)$$

K is constant and $K = \frac{1}{2\pi r}$

$$\therefore \sigma' \propto \frac{F}{b} \quad (3.34)$$

Where,

F = force, N

A= area, mm^2

r = radius of the opening span radius, mm

b= thickness of specimen, mm

σ'=damage resistance strength, N/mm

Thus, damage resistance strength was obtained by dividing the force by the thickness of each composite.

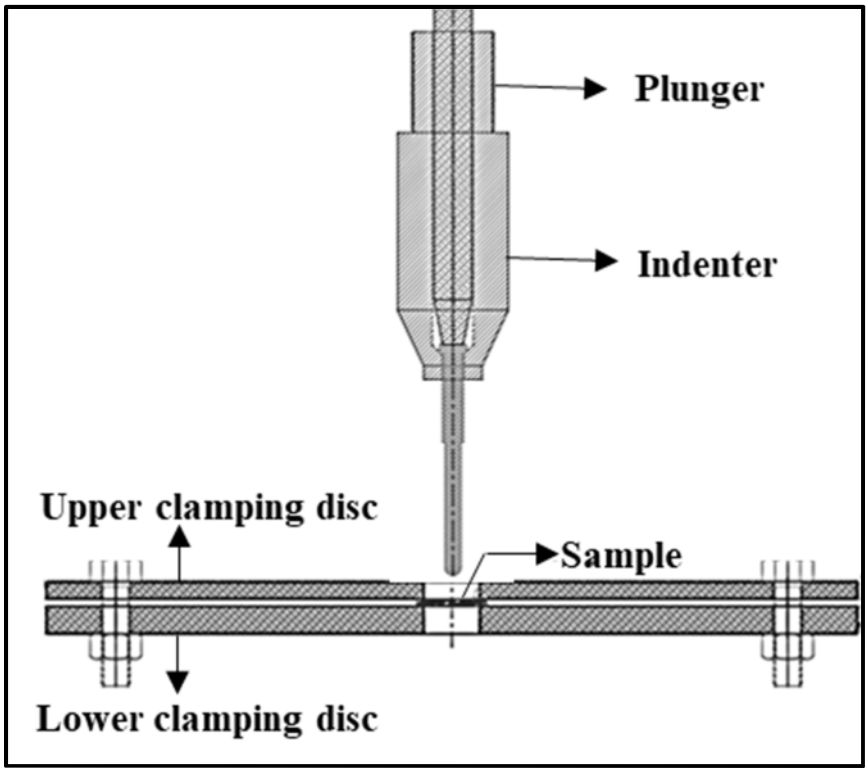

Figure 3.35: Schematic diagram of Quasi static indentation test set-up

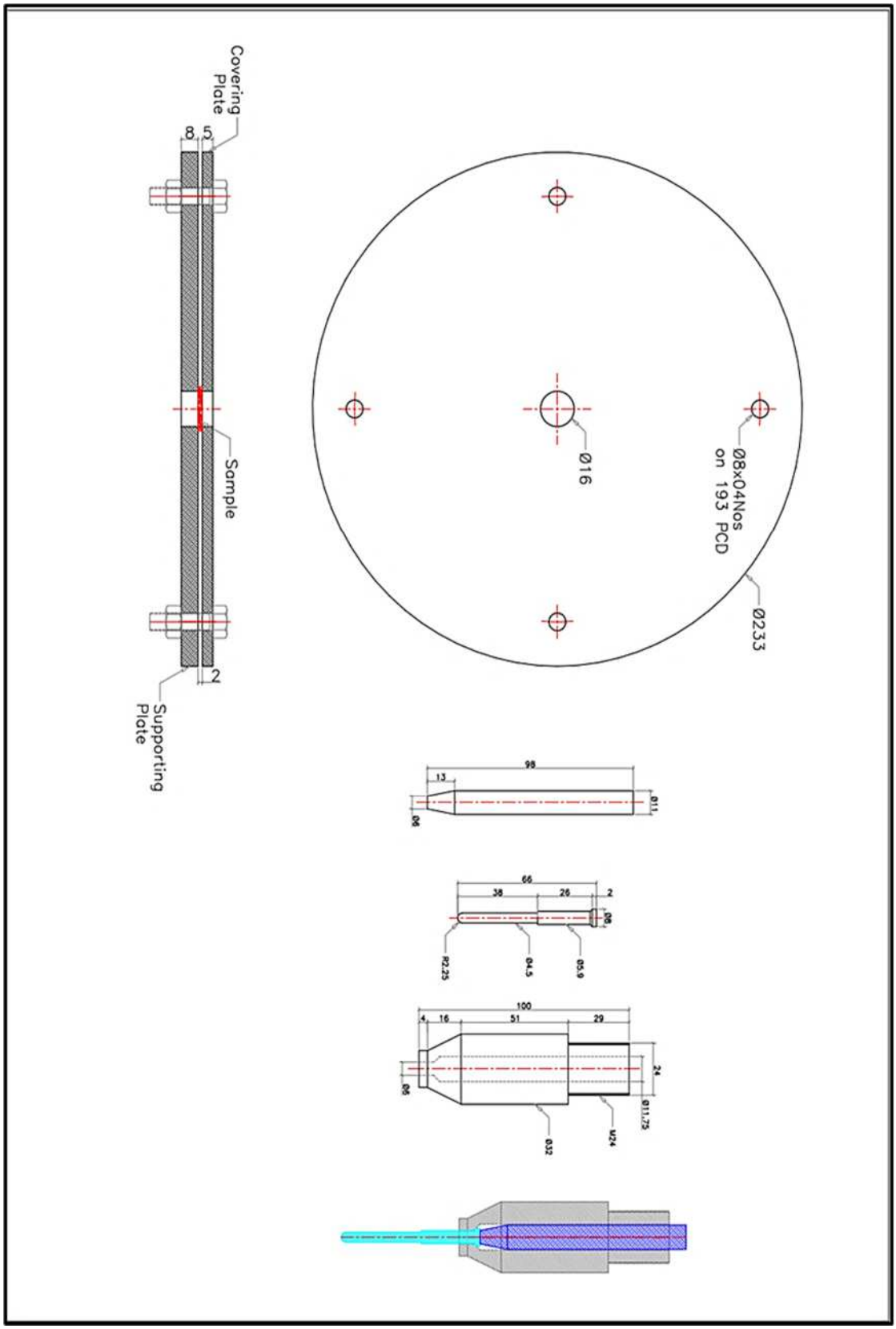

Figure 3.36: Schematic diagram of Quasi static indentation test apparatus

3.4.3 Fracture analysis

3.4.3.1 Scanning Electronic Microscope (SEM)

Figure 3.37: Scanning Electronic Microscope

The mechanical properties are directly associated to their structure. Moreover, the macroscopic failure is more dependent on microscopic damage mechanism. In this study, the fractured surface of the representative specimen, tensile, flexural, Izod impact and quasi static indentation test, were examined using Scanning Electronic Microscope (SEM). The instrument used for this work was SEM-SU1510 (Hitachi Company, Tokyo, Japan) as shown in Figure 3.37. The parameters for scanning the image were: resolution [3.0 nm at 30 KV (High Vacuum Mode),4.0 nm at 30 KV (Variable Pressure Mode)], magnification (x5

to x300,000) and electron gun accelerating voltage (0.3 to 30 KV). Throughout the work filament was kept same i.e. Tungsten filament. The images obtained by SEM are recorded and analysed in Chapter 4.